New Phytologist

Methods

Leaf gas exchange measurement for steady-state stomatal conductance model calibration

Kyle T. Rizzo, Tong Lei, Thomas N. Buckley and Brian N. Bailey

Department of Plant Sciences, University of California, Davis, Davis, CA 95616, USA

Author for correspondence:
Brian N. Bailey
Email: bnbailey@ucdavis.edu

Received: *4 November 2025*
Accepted: *22 December 2025*

New Phytologist (2026) **250:** 672–690
doi: 10.1111/nph.70949

Key words: gas exchange, model calibration, porometer, protocol, stomatal conductance.

Summary

- Stomatal conductance models are essential components of crop and land surface models, but collecting data to calibrate them remains challenging due to large leaf-to-leaf variability, slow stomatal kinetics, and a lack of consistent measurement protocols, leading to unknown reliability and representativeness of calibrated model parameter estimates.
- We combined field measurements, 3D biophysical simulations, and statistical power analyses to quantify parameter calibration discrepancies with different instruments under different conditions to provide recommendations for protocol development.
- Leaf-to-leaf physiological variability in measured steady-state stomatal conductance exceeded threefold under identical conditions, calling into question the use of few steady-state response curves to represent a canopy. Stomatal kinetics introduce systematic error in parameter calibration, and slower stomatal response times necessitated larger survey sample sizes to recover known stomatal model parameters of simulated data.
- Primary recommendations are as follows: survey measurements (*c.* 100 samples) are needed to sample leaf-to-leaf variability and can be supplemented by steady-state measurements to better represent environmental responses, survey measurements should maximize the range of leaf-level environmental conditions while minimizing transient effects, and steady-state measurements with controlled environmental conditions should maintain constant conditions for 15–45 min before measurement to allow for true stomatal steady state and not just instrument equilibrium.

Introduction

To supply CO_2 for photosynthesis, plant leaves have microscopic pores in their protective outer epidermal layer called stomata that readily enable gas exchange with the ambient environment. Stomatal pores open to acquire carbon dioxide and, in exchange, expose moist internal cells to the comparatively dry atmosphere, leading to rapid water loss. In order to manage this water loss and avoid desiccation, the aperture of stomatal pores is passively and actively regulated in response to a range of environmental stimuli, primarily absorbed light and leaf water status. This stomatal regulation influences plant productivity, water use efficiency, and global carbon and water cycles, thereby impacting agriculture, ecosystem health, and plant-based climate change mitigation (Willmer & Fricker, 1996; Jones, 1998; Hetherington & Woodward, 2003; Bertolino *et al.*, 2019; Faralli *et al.*, 2019; Gray & Dunn, 2024).

The degree to which stomata allow the diffusion of water vapor out of the leaf is most commonly quantified in terms of stomatal conductance (or its reciprocal, stomatal resistance). The total conductance to water vapor is defined mathematically as the ratio of the leaf evaporative water vapor flux (transpiration) to the difference in water vapor mole fraction between the leaf interior air spaces and the air immediately outside of the leaf boundary layer. Stomatal conductance is one of three conductances that are typically accounted for in the total conductance between a leaf's internal air space and the atmosphere, along with cuticular and boundary-layer conductances (Farquhar & Sharkey, 1982). Cuticular conductance is generally assumed to be negligible, in which case stomatal conductance is then computed as the reciprocal of the difference of total resistance and boundary-layer resistance (Buckley *et al.*, 1999).

Several decades ago, commercially available instrumentation facilitating rapid measurement of stomatal conductance became widely available, which transformed our ability to quantify and understand stomatal responses across species and environmental regimes. This began with the advent of the porometer (Weatherley, 1966; Shimshi, 1977; Rebetzke *et al.*, 2000), which estimates stomatal conductance under the instantaneous environmental conditions experienced by the leaf at the time of measurement.

Later, portable gas exchange systems were developed (Parkinson *et al.*, 1980; Field *et al.*, 1982; Atkinson *et al.*, 1986), which can estimate stomatal conductance under natural environmental conditions, as well as instrument-regulated artificial environmental conditions generated insidethe measurement chamber. Each of these instruments and approaches has trade-offs in terms of stomatal conductance measurement, which will be discussed in detail throughout this article.

Despite the wide availability of instrumentation for measuring stomatal conductance, these measurements are still relatively tedious and provide only a limited representation over time and space. In order to interpolate and extrapolate available measurements, numerous mathematical models of stomatal conductance have been developed to predict stomatal behavior based on specified environmental conditions (Damour *et al.*, 2010; Buckley, 2017). While there are a wide range of approaches for modeling stomatal conductance, ranging from cellular to ecosystem scales, this work focuses on steady-state leaf-level models that predict stomatal conductance on a leaf surface area basis as a function of local microclimatic conditions, which can then be upscaled using various types of canopy transfer models (e.g. Wang & Jarvis, 1990; Leuning *et al.*, 1998; Oleson *et al.*, 2010). This class of stomatal conductance model is a critical component of land surface models (Oleson *et al.*, 2010), crop models (Jones *et al.*, 2003), and basic physiological research seeking to understand mechanisms underpinning stomatal function (Buckley *et al.*, 2003).

In order for stomatal conductance models to be applied within the context of a specific plant system, model parameters must be calibrated based on measurements in that system. While the instrumentation for measuring leaf-level stomatal conductance (model output) along with relevant environmental conditions (model inputs) exists, reliably estimating these parameters based on *in situ* gas exchange measurements is complicated by a number of factors. Stomatal conductance and associated leaf-level environmental inputs are highly variable – they vary across the subleaf through whole-plant spatial scales and across subminute through seasonal temporal scales (Mott & Buckley, 1998). Furthermore, stomata can be relatively slow to respond to changes in environmental conditions, with typical lags of 15–60 min or more (Vialet-Chabrand *et al.*, 2017). Thus, stomata are often not in equilibrium with their environment at the time of measurement, making it difficult to use such measurements to calibrate a steady-state model without significant wait time.

Despite these known issues in stomatal conductance measurement for steady-state model calibration, they are often not considered or discussed in the literature reporting or using stomatal conductance model parameter values. Additionally, associated errors in estimated parameter calibrations are not generally well-understood or quantified, prohibiting the development of efficient measurement protocols that maximize model performance. With these gaps in mind, this work sought to evaluate various approaches for stomatal conductance measurement at the leaf level for canopy-averaged model parameter calibration in order to better quantify their differences and ultimately develop generalized recommendations (Fig. 1). Multiple instrument types were evaluated, along with sampling strategies across a range of spatiotemporal scales. In order to supplement limited field measurements, a leaf-resolving 3D biophysical model was used to simulate measurements and disentangle the variability in stomatal conductance due to environmental fluctuations from the variability caused by differences in the underlying physiological parameters that govern stomata.

Specifically, we aimed to answer the following questions:

(**1**) *Spatial and temporal variability*: Which spatial and temporal sampling strategies lead to derived stomatal conductance parameters that are representative of average whole-plant and canopy behavior?

(**2**) *Nonsteady-state effects*: How do variable stomatal response kinetics affect the calibration of popular steady-state stomatal conductance models? And how can their effects be mitigated in nonsteady-state survey measurements?

(**3**) *Instrument trade-offs*: What are the practical implications of using porometers vs portable gas exchange systems for stomatal conductance model calibration with regard to cost, efficiency, and reliability?

Stomatal physiology

External and internal stimuli Stomata function as evolutionarily optimized feedback controllers that govern a leaf's carbon and water exchange. Thus, any environmental variable that causes a change in the leaf's carbon and water balance is likely to induce a stomatal response. The variables that explain the bulk of stomatal response to environmental perturbations (and thus typically the primary input variables in stomatal conductance models) are light (photosynthetic photon flux density; PPFD) (Sharkey & Raschke, 1981; Shimazaki *et al.*, 2007) and evaporative demand (leaf-to-air vapor pressure difference; VPD) (Buckley, 2005, 2019; Zhou *et al.*, 2013; Grossiord *et al.*, 2020). These quantities are commonly obtained with nondestructive measurements in direct coordination with stomatal conductance measurement on the same instrument (Fig. 2), as with the LI-600 porometer and LI-6800 portable gas exchange system (LI-COR Biosciences, Lincoln, NE, USA), CIRAS-4 (PP Systems, Amesbury, MA, USA), and LCpro T (ADC BioScientific Ltd, Hoddesdon, Hertfordshire, UK). Instruments that provide stand-alone stomatal conductance measurement such as the SC-1 (Meter Group, Pullman, WA, USA) and AP4 (Delta-T Devices, Burwell, Cambridgeshire, UK), porometers can be coupled with independent photosynthetically active radiation sensors, psychrometers, and thermocouples for similar data collection.

Several other variables, including those internal to the leaf, also govern the stomatal response (Lawson & Matthews, 2020) but require destructive measurements or are difficult to obtain as independent model inputs, so are often inferred from data using inversion techniques or estimated from noncoincidental measurements. These include guard cell turgor pressure, epidermal turgor pressure, osmotic potential, total water potential (Buckley *et al.*, 2003), intercellular hormone concentrations, particularly abscisic acid (Acharya & Assmann, 2009; Mansfield, 2012;

New Phytologist

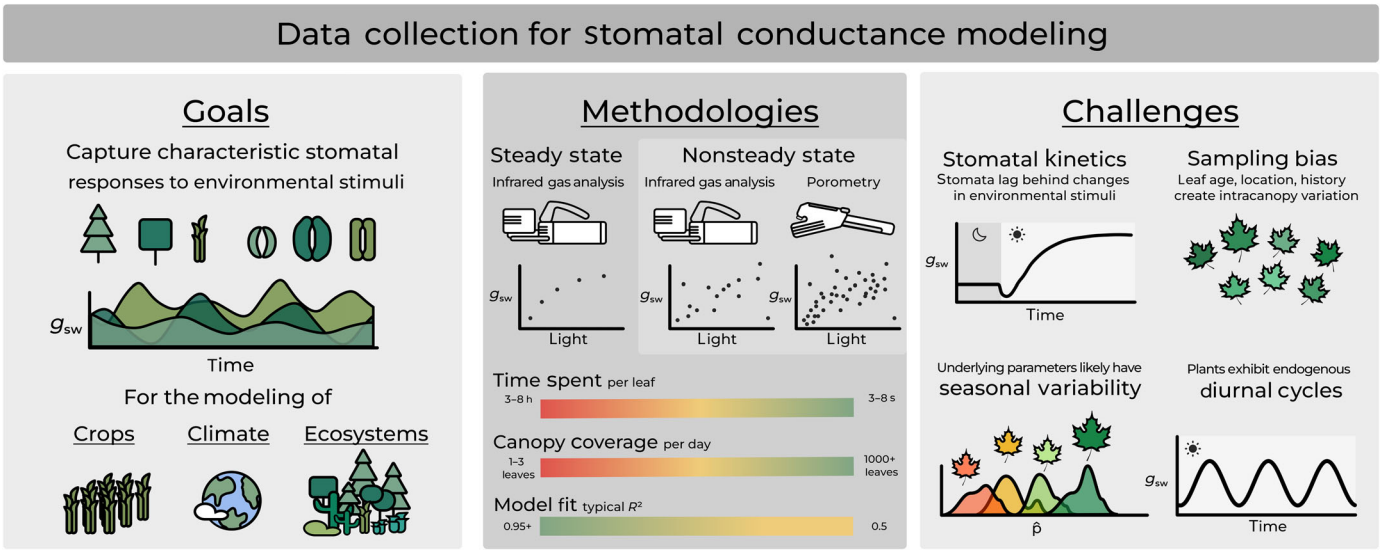

Fig. 1 Calibrating stomatal conductance (g_{sw}) models often has the goal of characteristically representing different species or broad plant functional types via the speed, shape, and scale of their responses to environmental stimuli. Two common instruments for data collection to be fed into models include portable gas exchange systems and porometers, which exhibit key trade-offs. In addition to limited instrumentation, several biological factors complicate the data collection of stomatal conductance including, but not limited to, variable stomatal kinetics, intracanopy variation, seasonal effects, and endogenous dynamics such as hormonal cycles, nutrition, or aging that are difficult to represent in stomatal conductance models. Note that graphical depiction of instruments were chosen based on commonly used and recognizable models but are not meant to promote any one model over another.

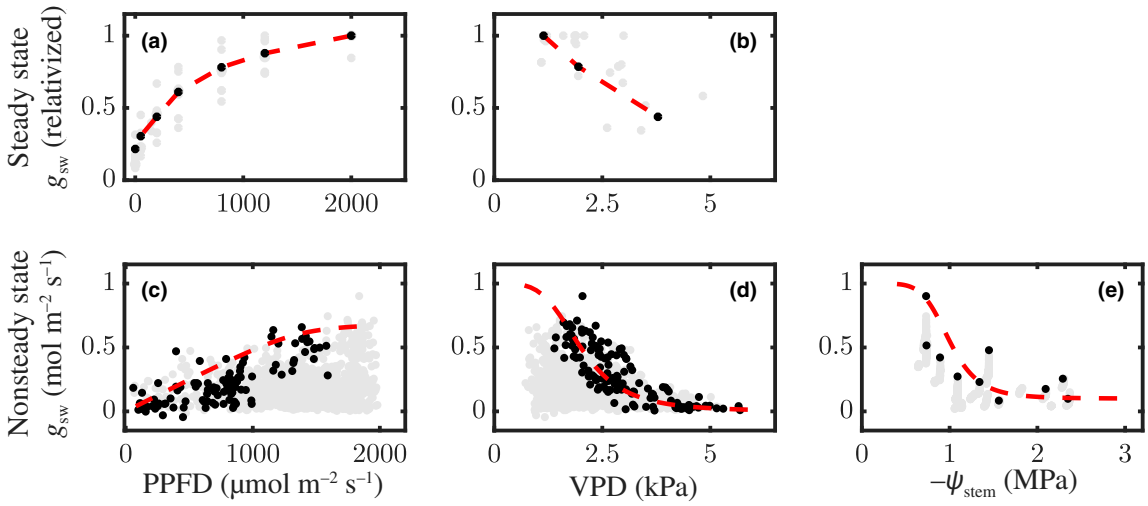

Fig. 2 Typical steady-state and nonsteady-state stomatal measurements and their correlations with environmental variables (red lines). All data (gray points) are a collection of many tree species, native and cultivated. In the steady-state light and vapor pressure deficit (VPD) response plots (a) and (b), a single species is highlighted (black points). In (e), the maximum stomatal conductance (g_{sw}) for a given stem water potential (ψ_{stem}) is highlighted (black points). Data were collected over many years using methods similar to the steady-state, nonsteady-state, and pressure chamber methods described in the Materials and Methods section.

McAdam & Brodribb, 2015), transmembrane ion fluxes (Fan *et al.*, 2004; Nilson & Assmann, 2007), intercellular CO_2 concentration (Mott, 1988), and differential light quality (Matthews *et al.*, 2020; Bernardo *et al.*, 2023).

Stomatal response kinetics Stomata are relatively slow to respond to changes in external environmental conditions, with characteristic response timescales of 15–60 min or more (Iino *et al.*, 1985; Lawson *et al.*, 2011; Drake *et al.*, 2013; McAusland *et al.*, 2016). The characteristic shape of the time response is that of an exponential or sigmoidal function (Vialet-Chabrand *et al.*, 2017). Significant variation in the time to reach steady state exists between species (Zhang *et al.*, 2022) and within species (Vialet-Chabrand & Lawson, 2019). Fig. 3 illustrates typical gas exchange time series data logged during the acquisition of steady-state stomatal response curves and demonstrates that the time to reach steady state under the same conditions can vary twofold between species, here *c.* 15 and 30 min.

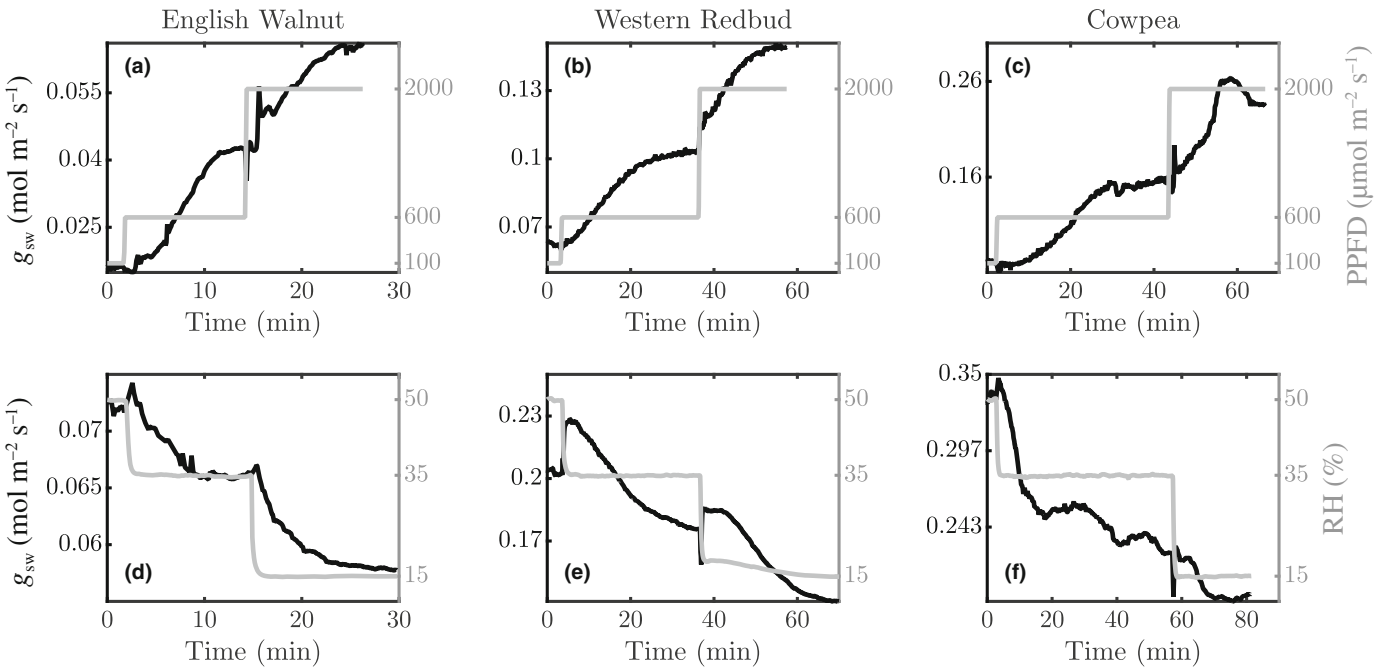

Fig. 3 Typical stomatal conductance (g_{sw}) response time series using the LI-COR LI-6800 portable gas exchange system. Light responses are shown in (a), (b), (c) and relative humidity (therefore, leaf to air vapor pressure difference) responses are shown in (d), (e), (f). Responses of English walnut (*Juglans regia*) are shown in (a), (d), of western redbud (*Cercis occidentalis*) in (b), (e), and of cowpea (*Vigna unguiculata*) in (c), (f). Note the difference in timescales on the x-axis between the three species. The measurement methodology used to collect this data is described in the Materials and Methods section. PPFD, photosynthetic photon flux density; RH, relative humidity.

The response times to different environmental stimuli such as light and VPD appear to be similar in angiosperms (Fig. 3; Grantz & Zeiger, 1986). Slow and species-specific stomatal kinetics complicate the calibration of stomatal conductance models with steady-state and nonsteady-state measurements because of the burdens of time and uncertainty that it adds. Beyond slow but monotonic stomatal kinetics, additional complexities exist such as oscillatory behavior (Cowan, 1972; Cardon *et al.*, 1994; Marenco *et al.*, 2006; Steppe *et al.*, 2006), circadian rhythms that appear to inhibit typical environmental responses (Hennessey *et al.*, 1993; Dodd *et al.*, 2005; Harmer, 2009; de Resco Dios *et al.*, 2013, 2016, 2020; Sun *et al.*, 2023), asymmetric time constants of stomatal opening and closing (Kirschbaum *et al.*, 1988; Ooba & Takahashi, 2003; McAusland *et al.*, 2016), and the so-called wrong-way response to an increase in transpiration resulting from an initial loss of water and turgor pressure from epidermal cells causing a temporary relief of pressure exerted on and further opening of the stomatal guard cells (Cowan, 1972; Kappen *et al.*, 1987; Buckley, 2005).

Spatiotemporal variability Plant canopies are made up of a consortia of leaves, each leaf with an individual, three-dimensional location and orientation that absorbs, reflects, and transmits incoming radiation. Individual leaf and subleaf fluxes exhibit much more variation than their canopy-scale equivalents. For example, due to the shading among leaves and the scattering of light, the fluxes of light on leaf surfaces often follow chaotic trajectories with abrupt changes (sunflecks and shadeflecks; Chazdon & Pearcy, 1991), compared with a smoother whole-canopy light interception trajectory (Fig. 4). Stomatal conductance at the leaf or subleaf scale is a function of the incident PPFD on individual leaves or subleaf patches and thus varies widely in both time and space due to sunfleck dynamics. This rapidly varying leaf-level environmental forcing, combined with the slow response kinetics described previously, means that stomata are often not in steady-state equilibrium with their environment at any instant (Kirschbaum *et al.*, 1988; Rayment *et al.*, 2000; Ozeki *et al.*, 2022).

Physiological variability The underlying stomatal characteristics that give rise to the speed, shape, and scale of stomatal responses to environmental cues vary across the population of leaves in a canopy (Vialet-Chabrand & Lawson, 2019), as is observed with other hydraulic parameters (Anderegg, 2015; Browne *et al.*, 2023). Leaf age, developmental history, microclimatic acclimation, seasonality, and other unaccounted-for physiological differences affect stomatal conductance (Frank, 1981; Vos & Oyarzun, 1987; Hiyama *et al.*, 2005; Matsumoto *et al.*, 2005; Maruyama & Kuwagata, 2008; Crous *et al.*, 2025) and lead to a distribution of stomatal characteristics within a canopy. Gas exchange measurement protocols for model parameter estimation could consider each parameter as a distribution and attempt to estimate this distribution (and perhaps its relationship to age and microenvironmental conditions within the canopy), but time and instrument expense often prohibit this scale of measurement from being feasible in practice.

New Phytologist

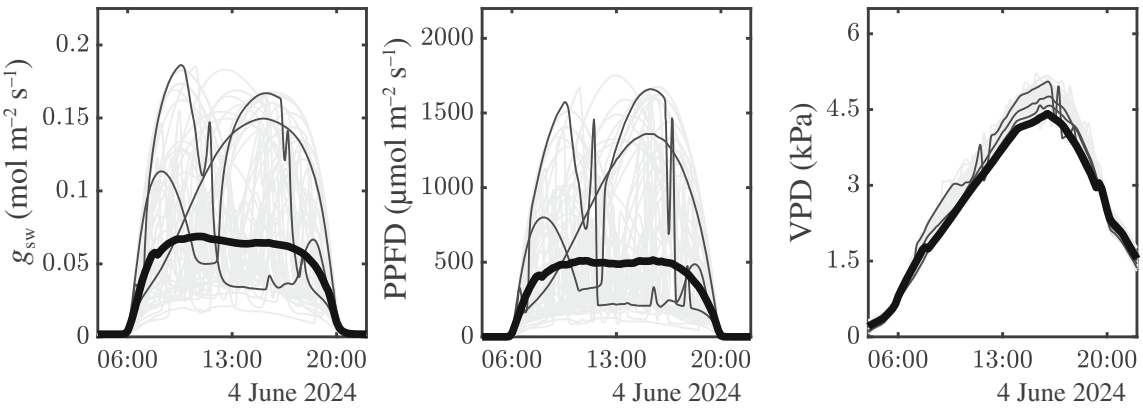

Fig. 4 Trajectories of modeled stomatal conductance (g_{sw}), incident photosynthetic photon flux density (PPFD) and leaf-to-air vapor pressure difference (VPD) of 50 random leaves (gray), three highlighted leaves (black), and the canopy average (bold black) within a virtual 3D canopy using a calibrated eastern redbud (*Cercis canadensis*) stomatal conductance model in the biophysical plant simulation library Helios.

Leaf gas exchange instrumentation

Porometer measurements Porometers use measurements of the change in water vapor in a chamber (cuvette) due to the presence of a transpiring leaf to estimate the associated stomatal conductance (McDermitt, 1990). They notably do not estimate CO_2 fluxes and thus do not give a measurement of photosynthetic assimilation. Different instrument manufacturers use different approaches for porometer design, but they are usually based on relatively inexpensive temperature and relative humidity sensors. In addition to being relatively inexpensive, contemporary porometers can also utilize a small air volume in the leaf chamber leading to rapid measurement stabilization, facilitating high measurement rates (100+ measurements per hour). A drawback of porometer instruments is that they typically do not have environmental control. This means that stomata are roughly at their natural state at the time of measurement, which is often not in equilibrium with environmental conditions given that the leaf-level environment (light, leaf temperature, air temperature, humidity, etc.) can change much faster than stomata can respond, such as when a shadow passes over the leaf. While most instruments have sensors that simultaneously record environmental variables (PPFD, air temperature, air humidity, and leaf temperature) at the time of measurement, this may not be representative of the effective steady-state environment that maps to the measured stomatal conductance value. This is problematic for steady-state model calibration because this process necessitates knowledge of the input environmental conditions corresponding to the output stomatal conductance value. An additional minor drawback to porometer-based measurements is that they usually only give the conductance for one side of the leaf per measurement, which means that multiple measurements per leaf may be necessary for amphistomatous species (Mott & O'Leary, 1984).

IRGA-based gas exchange measurements Portable gas exchange systems estimate stomatal conductance based on measurements of air water vapor concentration using infrared gas analyzers (IRGAs). By measuring the water vapor added to a cuvette chamber containing a leaf (along with other supporting measurements), stomatal conductance can be inferred, along with estimates of CO_2 fluxes and photosynthetic carbon assimilation. IRGAs are a relatively accurate means of measuring air water vapor concentration and thus an accurate means of measuring the transpiration flux into the cuvette, but they are quite expensive, bulky, require substantial expertise to operate, and have a number of warm-up tests and recommended best practices that make their usage time-consuming (Busch *et al.*, 2024). The main advantage of this type of instrument for measuring stomatal conductance is that it generally allows for precise environmental control inside the cuvette. Contemporary instruments allow for control of light, air temperature, air humidity, carbon dioxide concentration, and to a limited degree, boundary-layer conductance inside the leaf chamber. Thus, assuming that sufficient time has passed to allow for stomata to be in equilibrium with the chamber environment, a mapping can be recovered between input environmental conditions and output stomatal conductance, which is ideal for stomatal conductance model calibration.

There are several timescales associated with leaf gas exchange measurement that users should be aware of. After the environmental parameters have been set and the cuvette chamber has been closed on the leaf, the instrument and plant do not respond instantaneously. First, the instrument must adjust the environmental conditions to achieve the set points specified by the user, which may include adjusting the light flux (which is virtually instantaneous) or adjusting the air temperature or humidity, which can take several minutes. Once the instrument environmental set points have been achieved, there is an additional period required for the chamber water vapor flux to come to equilibrium, which may take 1–3 min or longer in some cases. At this point, the measurement is sufficiently stable to record the stomatal conductance based on the conditions the leaf experienced before the start of measurement (approximately). However, importantly, the stomata are most likely not at steady state with the environmental conditions of the chamber at this point,

which often requires much more time to achieve. It may take an additional 15–60 min or more for the stomata to reach steady state in response to new environmental conditions, even if the measurement appears 'stable' across a timescale of minutes (Fig. 5). In some cases, such as species with high hydraulic capacitance, stomatal conductance may oscillate for hours before reaching steady state (Cardon *et al.*, 1994; Marenco *et al.*, 2006; Steppe *et al.*, 2006).

Survey vs steady-state measurements Leaf gas exchange instruments can be applied using a nonsteady-state or 'survey' sampling strategy, or at steady state with known, controlled environmental conditions. For the purposes of steady-state model parameter calibration, it is ideal to have the plant in approximate equilibrium with its environment, such that the set of environmental variables can be mapped to a unique stomatal conductance state. If such equilibrium conditions do not exist, the set of measured environmental variables does not necessarily uniquely map to the current stomatal conductance state at the time of measurement.

The environmental control associated with IRGA-based leaf gas exchange instruments allows for stomatal measurement at approximate steady state, thus providing an ideal measurement for stomatal conductance model parameter calibration. The user can set the desired environmental variable set, and after waiting for stomatal steady state, record the stomatal conductance value based on equilibrium with that environment. By performing repeated steady-state measurements on the same leaf, users can systematically vary specified environmental conditions and generate smooth response curves that commonly result in excellent model fits (Fig. 6).

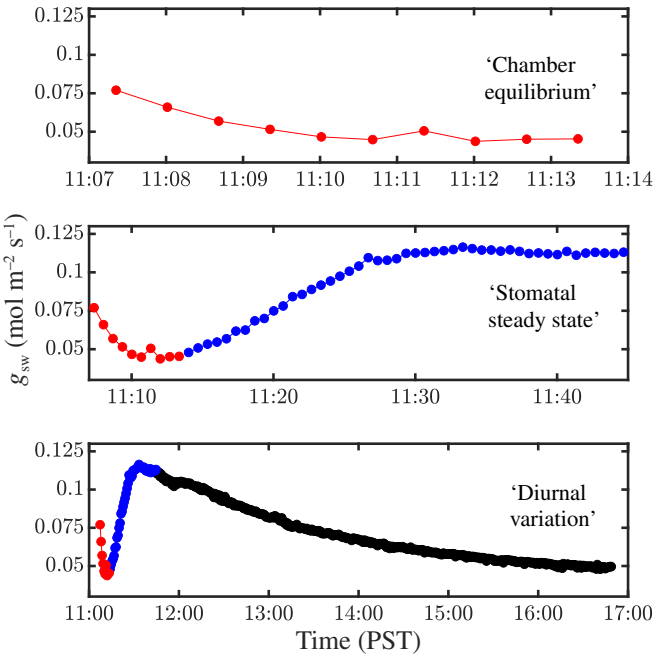

Fig. 5 Demonstration of the three timescales apparent in 'steady-state' stomatal conductance (g_{sw}) data collection. A single leaf of Texas red oak (*Quercus buckleyi*) was clamped into a LI-COR LI-6800 chamber from 11:00 to 17:00 PST with a constant photosynthetic photon flux density (PPFD) of 1600 μmol m^{-2} s^{-1}, T_{air} of 22°C and relative humidity (RH) of 35%. First, 'chamber equilibrium' is reached on the order of minutes and a stable measurement can be taken. Importantly, however, stomata have not reached 'stomatal steady-state' in response to chamber conditions, which took *c.* 25 min. Finally, underlying 'diurnal variation' occurred, likely due to changes in whole-plant water status, circadian rhythm, or other effects leading to stomatal closure despite constant PPFD and vapor pressure deficit over the next 6 h, reducing stomatal conductance by 50%.

As introduced previously, each steady-state measurement is time-consuming (*c.* 15–60 min each) and thus limits leaf-to-leaf measurement coverage. In a single day of measurement, it may only be possible to collect steady-state response curves for a few leaves. Results are thus prone to sampling bias, as resulting model parameters may be highly dependent on which leaves happened to be sampled.

On the other hand, survey measurements are relatively fast and enable efficient spatial sampling of leaves in the canopy. Porometer measurements can be taken in a few seconds to a minute, depending on the instrument used. IRGA-based gas exchange instruments, which generally have a larger cuvette volume, still require 30–60 s for each survey measurement but are fastest when the device is set to target reference, not sample (chamber) conditions, and provided the ratio of flow rate to chamber volume is high enough to quickly reach chamber equilibrium (but notably, not stomatal steady state). Thus, hundreds of survey measurements can be collected in a single sampling session, allowing for characterization of leaf-level variability across the canopy.

For survey measurements, variability is largely driven by leaf-level differences in microenvironmental conditions. Since the environmental conditions experienced by the leaf are not specified by the user, onboard sensor measurements of incoming PPFD, air temperature, air humidity, and leaf temperature can be used to provide inputs needed for model fitting. The drawback of the survey approach is that stomatal conductance as a function of environmental variables is very noisy with two components that are difficult to disentangle: variability in leaf-to-leaf microenvironmental conditions and variability in leaf-to-leaf underlying physiological parameters. The transient stomatal conductance state can exhibit dramatic mismatches with its environmental conditions such as when a leaf has moved from sunlight to shade just before the measurement is collected and stomata are still wide open. That measurement will erroneously associate low light with high stomatal conductance. It remains unclear what the balance looks like between the increased sample number afforded by survey measurements and the uncertainty introduced by nonsteady-state stomatal kinetics, and how many survey measurements are sufficient to come within an acceptable error tolerance with the underlying steady-state stomatal parameters.

Stomatal conductance models

The goal of stomatal conductance models is to both describe understood stomatal phenomena in observed data (interpolation) and generalize beyond observed data to predict stomatal

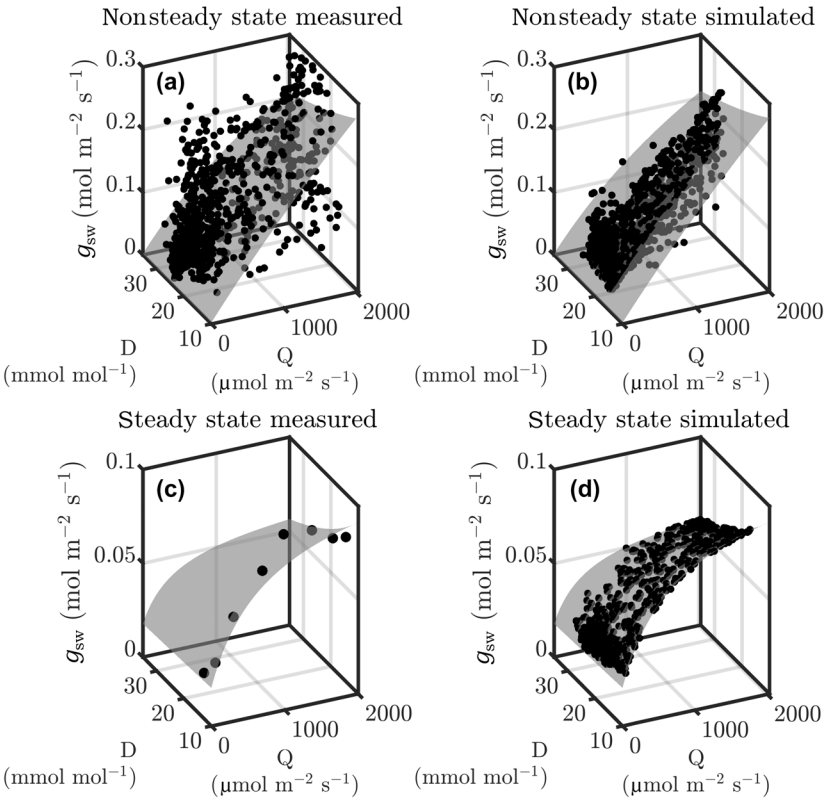

Fig. 6 Stomatal conductance (g_{sw}) measurements and model fits of eastern redbud (*Cercis canadensis*) under steady-state and nonsteady-state. Steady-state measurements were made on a single leaf using the LI-COR LI-6800, with a full stomatal response time of *c.* 45 min. Nonsteady-state measurements were made on hundreds of leaves at random of the same tree over a whole day using the LI-COR LI-600 porometer. The model surface in each case is the best-fit Buckley, Turnbull, Adams (BTA; 2012) model to the measured data in each case. Simulated data were generated from a 3D virtual canopy of hundreds of leaves with realistic ray-traced light fluxes (*Q*) and computed water vapor mole fraction differences (*D*). The steady-state simulation uses the BTA stomatal conductance model to generate g_{sw} from *Q* and *D* values while the nonsteady-state simulation adds to that a stomatal time-constant-limited approach to steady-state (time lag) and leaf thermal capacitance (heat storage).

conductance in new scenarios (extrapolation). Models of stomatal conductance have been developed and deployed in different scientific disciplines for different purposes. Plant physiologists and biologists have tended to develop models to support theories and test hypotheses of underlying mechanisms of stomata (Buckley, 2005; Nguyen *et al.*, 2023; Peak *et al.*, 2023), while agricultural scientists, ecohydrologists, and meteorologists have employed simplified models (Bassiouni & Vico, 2021; Grisafi *et al.*, 2022; Sabot *et al.*, 2022) for incorporation into crop models, land surface models, and large earth system models such as the Community Earth System Model (Kay *et al.*, 2015). Reviews of stomatal conductance models can be found in Damour *et al.* (2010) and Buckley (2017). We focus on single-equation, analytically solvable, steady-state models that can be empirically calibrated from field gas exchange data. Each model has a set of parameters with values likely varying across species, time, and space that must be accurately estimated in order to use the model in a given application.

Below, we highlight some of the most commonly used semi-empirical, steady-state stomatal conductance models used in agricultural and earth system applications.

Ball–Woodrow–Berry Model (1987) The Ball–Woodrow–Berry (BWB) or 'Ball–Berry' model (Ball *et al.*, 1987) of stomatal conductance is among the most widely used because of its perceived simplicity, particularly when using coincidental gas exchange measurements of net photosynthesis and stomatal conductance g_{sw}. The BWB model is typically written as

$$g_{sw} = g_0 + g_1 \frac{Ah}{C_a} \quad \text{Eqn 1}$$

where A is net photosynthesis (μmol m^{-2} s^{-1}), h is the relative humidity at the leaf surface (unitless), and C_a is the ambient air CO_2 concentration (μmol mol^{-1}). The parameters of this model are g_0 (mol m^{-2} s^{-1}) and g_1 (unitless).

Ball–Berry–Leuning Model (1995) Leuning (1995) replaced the linear humidity dependence in the BWB model with the term $\left(1 + \frac{\text{VPD}}{\text{VPD}_0}\right)^{-1}$, which has a nonlinear dependence on the vapor pressure deficit, VPD (kPa), and augmented the CO_2 response with an offset, the CO_2 compensation point, Γ (μmol mol^{-1}). The Ball–Berry–Leuning model takes the form

$$g_{sw} = g_0 + g_1 \frac{A\left(1 + \frac{\text{VPD}}{\text{VPD}_0}\right)^{-1}}{C_a - \Gamma} \quad \text{Eqn 2}$$

Medlyn *et al.*'s optimality model (2011) The Medlyn *et al.*'s (2011) model, which sought to reconcile empirical and optimality-derived stomatal conductance models, has the form

$$g_{sw} = g_0 + 1.6\left(1 + \frac{g_1}{\sqrt{VPD}}\right)\frac{A}{C_a} \quad \text{Eqn 3}$$

This expression is derived from theory formalized by Cowan & Farquhar (1977), which postulates that stomata optimize carbon assimilation given a fixed water budget. It is a linearized analytical approximation to a constrained optimization problem that otherwise requires numerical iteration to solve completely. The assumptions used to reduce a complex numerical solution into a simple analytical one include a negligible boundary layer conductance, only RuBP-regeneration-limited photosynthesis (nonsaturating light conditions), and a decoupling of leaf temperature and stomatal conductance (Arneth *et al.*, 2002).

Buckley, Turnbull, Adams Model (2012) The Buckley, Turnbull, Adams (BTA) model presented in Buckley *et al.* (2012) sought to simplify a more explicit biohydromechanical model representing active and passive stomatal control (Buckley *et al.*, 2003). The simplified model lumps groups of physiological variables into semi-empirical parameters that can be readily determined from field data. Environmental inputs to the model are Q, the leaf absorbed PPFD ($\mu mol\, m^{-2}\, s^{-1}$), and D, the leaf water vapor mole fraction difference ($mmol\, mol^{-1}$; VPD divided by P_{atm}, the ambient pressure), and takes the form

$$g_{sw} = \frac{E_m(Q + i_0)}{k + bQ + (Q + i_0)D} \quad \text{Eqn 4}$$

The parameters E_m, k, b, and i_0 are treated as empirically fitted parameters in practice but do retain some intended physiological meaning. E_m represents the maximum transpiration rate as D approaches infinity and equals $K_l(\psi_{soil} + \pi_e)$, where K_l is the leaf specific hydraulic conductance ($mol\, m^{-2}\, s^{-1}\, MPa^{-1}$), ψ_{soil} is the soil water potential (MPa), and π_e is the epidermal osmotic pressure (MPa). i_0 determines the stomatal conductance in the dark at a given VPD. k primarily affects the shape of the light response and equals $\frac{K_l}{\chi\varphi}$, where χ is the guard cell turgor to conductance scalar ($mol\, m^{-2}\, s^{-1}\, MPa^{-1}$), and φ is the initial slope of the guard cell advantage light response ($\mu mol\, m^{-2}\, s^{-1}$). b primarily shifts the VPD response by shifting the D at which g_{sw} is half its maximum as Q approaches infinity and equals $\frac{K_l}{\chi\alpha_m}$, where α_m is the guard cell advantage at saturating irradiance.

Stomatal conductance modeled as a function of assimilation Many models, including three of the four we highlight here, calculate stomatal conductance as a function of photosynthetic assimilation rate, A (Damour *et al.*, 2010). This has proven historically successful in capturing this tightly coupled empirical relationship (Berry, 2012; Buckley, 2017). In most forward-modeling applications, A is not a measured input, but rather a modeled quantity alongside g_{sw}. A is most commonly modeled using the Farquhar–von Caemmerer–Berry model of photosynthesis (Farquhar *et al.*, 1980), which is a function of light, temperature, and the internal CO_2 concentration, C_i, and has between 10 and 20 free parameters that require their own separate calibration (Gu *et al.*, 2010; Wang *et al.*, 2014; Lei *et al.*, 2025). C_i is also not a measured quantity in applications of crop and land surface models, and so it too needs to be computed, and as a function of g_{sw}. This creates a set of coupled equations for A, g_{sw}, and C_i (e.g. Kim & Lieth, 2003; Jefferson *et al.*, 2017), which requires iteration to solve as well as photosynthetic parameters unique to the species being modeled. This greatly increases the total parameter count to model g_{sw} from 2–4 to $\gtrsim 10$ (stomatal and photosynthetic parameters) (Bernacchi *et al.*, 2001; Supporting InformationTable S1) and is especially inefficient in scenarios in which g_{sw}, temperatures, and transpiration are relevant but not photosynthetic assimilation (e.g. Krayenhoff *et al.*, 2020; Ponce de León & Bailey, 2021; Mayanja *et al.*, 2025). Models requiring A are also not amenable to calibration via a porometer alone, as porometers do not provide measurements of A. Approximations of A can be made with the porometer alone, particularly when equipped with additional instrumentation for performing fluorescence measurements but first require calibration using a portable gas exchange system (Kimura *et al.*, 2025). We demonstrate an approach to this approximation in Notes S1.

Materials and Methods

Stomatal conductance measurement

Several stomatal conductance data collection campaigns across 18 species (Table S2) were performed in the field (as described later) to illustrate issues and considerations relevant to performing measurements for stomatal conductance model fitting. The porometer used for survey measurements was the LI-COR LI-600 Porometer/Fluorometer (LI-COR Biosciences, Lincoln, NE, USA). Survey and steady-state measurements were conducted using the LI-COR LI-6800 Portable Photosynthesis System with the small light source chamber head (6800-02).

LI-6800 common settings For all measurements of stomatal conductance using the LI-COR LI-6800, some common settings were used across multiple campaigns. The chamber leaf area aperture was $2 \times 3\ cm^2$, the flow rate was 500 $\mu mol\, s^{-1}$, the chamber pressure differential was 0.1 kPa, and the fan speed was 10 000 rpm. Additional settings that differ between experiments are indicated where relevant.

Stomatal response kinetics For the measurement of stomatal response kinetics, two healthy, sunlit, fully expanded leaves of each of two mature tree species, English walnut (*Juglans regia*) and western redbud (*Cercis occidentalis*), were measured using a LI-COR LI-6800 in Davis, CA, USA, on 27 September 2024 and 12 October 2024, respectively, between 11:00 and 16:00 PST. Two step changes in light intensity were performed on one

leaf of each species, and two step changes in VPD were performed on the other leaf of each species. Leaves in the light responses were left to reach steady-state stomatal conductance at chamber conditions of 50% relative humidity, 25°C air temperature, and 100 μmol m^{-2} s^{-1} PPFD. Step changes to 600, and to 2000 μmol m^{-2} s^{-1} PPFD were then made. Leaves in the VPD responses were left to reach steady-state stomatal conductance at chamber conditions of 25°C, 2000 μmol m^{-2} s^{-1} PPFD, and 50% relative humidity. Step changes to 35% and to 15% relative humidity were then made.

Intracanopy steady-state variation Six leaves across two neighboring English walnut trees in a research orchard in Davis, CA, USA, were measured for their steady-state stomatal conductances from 10:00 to 16:00 PST on 27 September 2024. Leaves labeled as 1, 2, and 5 were on Tree 1, and Leaves 3, 4, and 6 were on Tree 2. Two LI-COR LI-6800s were used such that leaf pairs (1,2), (3,4), and (5,6) were measured parallel in time. Each leaf was subject to a steady-state stomatal light response followed by a steady-state stomatal VPD response. The sequence of chamber conditions for all leaves was (100, 600, 2000, 2000, 2000) μmol m^{-2} s^{-1} PAR, (50, 50, 50, 35, 15)% relative humidity, and (30, 30, 30, 30, 30)°C air temperature.

Spatiotemporal sampling A random sample of 25 sunlit leaves and 25 shaded leaves was measured every 2 h from 06:00 to 18:00 PST using a LI-COR LI-600 porometer on a single eastern redbud tree in Davis, CA, USA, on 3 June 2024 and again on 4 June 2024. Different slices of the hourly data were used to calibrate a stomatal conductance model, and their differences in fitted parameter values and modeled outcomes were evaluated.

Time in chamber test A leaf of a large Texas red oak (*Quercus buckleyi*) tree in Davis, CA, USA, was measured on 30 November 2023 from 11:00 to 17:00 PST and subjected to constant LI-6800 chamber conditions with a PPFD of 1600 μmol m^{-2} s^{-1}, T_{air} of 22°C, and RH of 35% (equating to a VPD of 17 mmol mol^{-1}). A mix of neighboring sunlit and shaded leaves were periodically measured in their ambient light over the same time period using an LI-600 porometer to compare of trends of diurnal g_{sw} inside and out of the chamber.

Stem water potential Stem water potentials, where reported, were measured with a Scholander pressure chamber from the average of two shaded, basally located leaves per tree per hour bagged with a Mylar bag for 30 min before excision and chamber measurement. Hourly measurements of each tree were made, and interpolated (Akima, 1970) for a continuous time series. From this time series, an average stem water potential $\overline{\psi}_{stem}$(MPa) was recorded for leaves during their time in the LI-6800 chamber by averaging over the time range corresponding to the respective leaf in the chamber. Midday stem water potential $\psi_{stem}^{12:00}$ (MPa) of individual trees was also estimated from these interpolations and reported where relevant.

Psychrometric correction of porometer stomatal conductance

Stomatal conductance as measured by porometers has been documented to diverge from the higher precision measurements made by portable gas exchange systems (Turner, 1991), particularly under high chamber relative humidity (McDermitt, 1990), large gradients in leaf to air temperature (Tyree & Wilmot, 1990), and large gradients in leaf to sensor housing temperature (Verhoef, 1997). All in all, this can lead to a 50–100% positive bias seen in porometer g_{sw} over IRGA-based g_{sw} (Lamoureux *et al.*, 2017; Toro *et al.*, 2019). We also observed this bias and have attempted to correct for it using a first principles approach, the details of which can be found in Rizzo & Bailey (2025b). All of the porometer data used for analysis in this work has had the correction applied to it, which, on average, reduces values by a factor of 1.5 but deviates from this average at very high and very low measured stomatal conductances.

Model fitting

Parameters of the BTA stomatal conductance model (Eqn 4) for each data group in question were fit using stochastic gradient descent implemented in a plant physiological model fitting library, PhoTorch (Lei *et al.*, 2025). In addition to minimizing the mean-squared error between observations and model predictions, the library adds a few constraints to the formulation to promote biologically reasonable results in particularly sparse datasets, namely a positive light response ($\frac{\partial g_{sw}}{\partial Q} > 0$) with negative curvature ($\frac{\partial^2 g_{sw}}{\partial Q^2} < 0$), a negative VPD response ($\frac{\partial g_{sw}}{\partial D} < 0$), and non-negative stomatal conductances ($g_{sw} > 0$). Fitting of all four models and their comparisons can be found in the Supplementary Information (Notes S2; Fig. S1; Tables S3–S6).

Simulated data generation

In order to better quantify and understand spatiotemporal variability in stomatal conductance, a three-dimensional (3D) biophysical plant model was used to simulate leaf-level variability in stomatal conductance. A virtual canopy allows for realistic subhourly fluctuations in leaf light interception and temperature due to sunflecks and shadeflecks resulting from other leaves in the canopy and sun's angle in the sky. The resulting stomatal conductances are then produced from exactly known steady-state parameters and environmental conditions, something not achievable at scale in reality. The model, Helios (Bailey, 2019), discretizes the 3D plant geometry into a mesh of rectangular or triangular planar elements that fully resolves the plant down to the subleaf scale. These primitive elements serve as the computational basis for model calculations, for which absorbed radiative fluxes in the PAR, NIR, and longwave bands are calculated, along with the element energy fluxes, surface temperature, leaf-to-atmosphere vapor pressure deficit, and ultimately stomatal conductance. A more complete description of the model is given in Notes S3; Fig. S2. Example modeled time-series trajectories of

stomatal conductance, PPFD, and VPD for individual leaves are shown in Fig. 4.

The simulations were run for 4 June 2024 using weather inputs from the CIMIS station (Brainard *et al.*, 1996) located in Davis, CA, USA. For the geometry, a 3D eastern redbud tree model was synthetically generated with the parametric, phytomer-based plant architecture framework available in Helios. Steady-state stomatal conductance was simulated using the BTA model described previously applied at the subleaf element level, with coefficients $E_m = 21.88$ (mmol m^{-2} s^{-1}), $i_0 = 11.47$ (μmol m^{-2} s^{-1}), $k = 138\,700$ (μmol m^{-2} s^{-1} mmol mol^{-1}), $b = 0$ (mmol mol^{-1}), obtained from fitting to steady-state stomatal response measurements. Nonsteady-state stomatal conductance was simulated using a time-lagged exponential approach to the steady-state value:

$$g_{sw}^{t+1} = g_{sw}^{t} + \left(g_{sw,ss}^{t+1} - g_{sw}^{t}\right)\frac{\Delta t}{\tau_{gsw}} \quad \text{Eqn 5}$$

where superscripts denote time indices, $g_{sw,ss}$ is the steady-state BTA model stomatal conductance, g_{sw} is the non-steady-state realized stomatal conductance, Δt is the timestep (s), and τ_{gsw} is the stomatal time constant (s), which is the time taken to reach $1-1/e$, or ≈63%, of the steady-state value.

Model performance metric

Comparisons of measured and modeled time series of average canopy values were performed using the refined index of agreement (d_r, unitless) proposed by Willmott *et al.* (2012), computed as

$$d_r = \begin{cases} 1 - \dfrac{a}{b}, & a \le b, \\ \dfrac{b}{a} - 1, & a > b, \end{cases} \quad \text{Eqn 6}$$

$$a = \sum_{i=1}^{n} \left| P_i - O_i \right|, \quad \text{Eqn 7}$$

$$b = 2\sum_{i=1}^{n} \left| O_i - \overleftarrow{O} \right|, \quad \text{Eqn 8}$$

where O_i are the observed values, P_i are the model predicted values, and $\overleftarrow{O}$ is the mean of the observed values. This metric has the properties of being bounded by −1 and 1, with 1 being a model that perfectly fits the observations, and −1 being a model that poorly fits the observations or a scenario in which the observations themselves do not vary about their mean.

Statistical analysis

A statistical power analysis was used to quantify the rate of successfully extracting model parameters within some threshold error of reference or 'true' parameters as a function of sample size (N). Simulated data of $N_{max} = 86\,140$ leaf patches were subsampled based on a sample size of N across a range of sample counts and each fit to BTA to determine its model parameters. For each subsample, a grid of stomatal conductance values was computed across a range of light and VPD inputs using the subsampled-derived extracted parameter set. Each grid was then compared with the grid generated from parameters derived from the full dataset using percent relative error (RE) computed as

$$\mathrm{RE} = \frac{1}{p}\sum_{i=1}^{p} \frac{\left| g_{sw,s_i} - g_{sw,S_i} \right|}{g_{sw,S_i}} \cdot 100 \quad \text{Eqn 9}$$

where g_{sw,S_i} is the BTA-modeled stomatal conductance for (flattened) grid location i calculated based on parameters fit from the full dataset S with sample size N_{max}, and g_{sw,s_i} is generated from parameters fitted from a subset of the data s with sample size N. Thus, when the sample size is equal to N_{max}, RE = 0.

The grids were compared across the domain of $Q : (0, 2000)$ and $D : (1, 50)$ with $p = 50^2$ total points. For each threshold (T) RE across a range from 0 to 100%, 1000 iterations (I) were performed, the number of RE below the threshold RE was tallied ($\mathbb{I}$), and success rates (S_T) were calculated as

$$S_T = \frac{1}{I}\sum_{i-1}^{I} \mathbb{I}(\mathrm{RE}_i < \mathrm{RE}_T) \cdot 100 \quad \text{Eqn 10}$$

Results

Intracanopy steady-state variation

Steady-state stomatal conductance was measured across a range of PPFDs and VPDs of fully expanded, healthy, sunlit leaves on the same trees, on the same day, to assess the degree to which the mapping from PPFD and VPD to steady-state stomatal conductance is conserved across leaves in a canopy. Measurements showed up to threefold differences in steady-state conductance under the same conditions, with some leaves reaching light-saturated, minimally VPD-stressed stomatal conductances of 0.05 mol m^{-2} s^{-1} and others 0.14 mol m^{-2} s^{-1} (Fig. 7).

This high leaf-to-leaf variation led to high variability in resulting g_{sw} model parameters, and the resulting simulated time course of modeled g_{sw} (Fig. 7) based on simplified input PPFD and VPD time courses. For some leaves, the fitted VPD responses were relatively weak, whereas for others, there was up to a 50% change in g_{sw} across a range in D of 20 to 50 mmol mol^{-1}. In the example simulated daily time course of g_{sw} shown in Fig. 7(c), some leaves exhibited a large midday depression in g_{sw} while others exhibited none. For estimation of downstream processes dependent on g_{sw} such as leaf temperature, transpiration, and photosynthetic assimilation, this variability would significantly influence their magnitude and diurnal pattern. This demonstrates the limitations of basing stomatal conductance model parameter estimates on a single or even a few leaves from a

New Phytologist

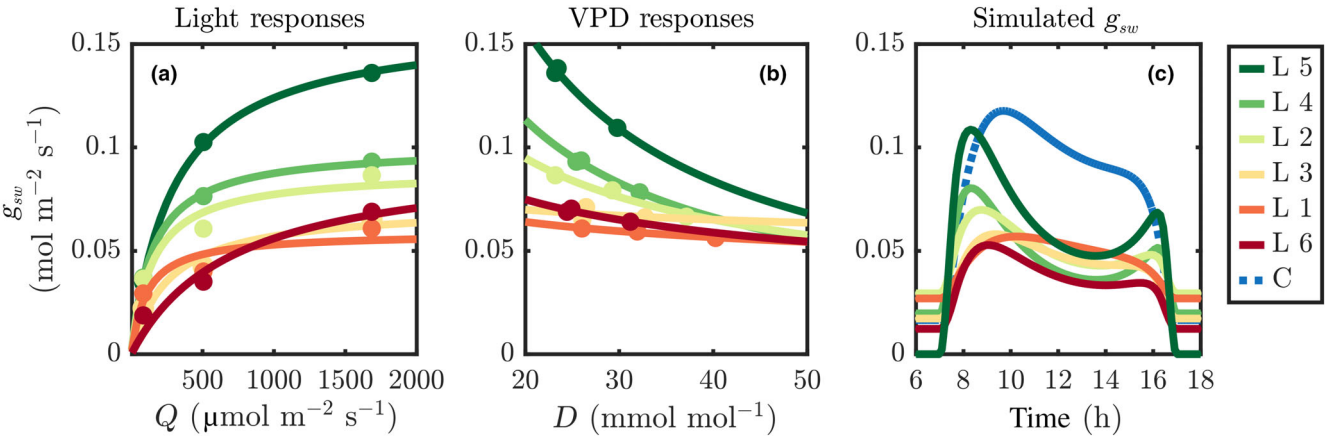

Fig. 7 Steady-state stomatal conductance (g_{sw}) response curves of six leaves (labeled 'L' 1–6) and one canopy ('C') of three neighboring English walnut (*Juglans regia*) trees over the course of one day. Leaves with 'L' were measured at steady state using the LI-6800, while the canopy 'C' was measured hourly at 50 leaves per hour with the LI-600 porometer. Extracted model parameters for each surface are listed in Table 1, where the canopy shown here is the Late Season parameter set. Data from each sampled leaf were used to fit the Buckley, Turnbull, Adams (2012) model of stomatal conductance. These data are plotted along single axes of light (as Q, the absorbed photosynthetic photon flux density (PPFD)) in (a) and vapor pressure deficit (VPD) (as D, the water vapor mole fraction difference) in (b) for comparison between leaves. In subplot (c), extracted best-fit model parameters for each leaf are used to show the modeled g_{sw} under a typical, simplified daily regime of PPFD and VPD, the two environmental inputs, exemplifying how leaf choice can significantly affect resulting calibrated model output, in magnitude and diurnal shape.

given species or genotype to characterize its stomatal conductance. Given the extreme throughput limitations of these steady-state measurements, it is unlikely that this type of measurement alone will be able to sufficiently capture both stomatal responses and leaf-to-leaf variability.

Representativeness of model parameters derived from varying sampling periods

The goal of gas exchange measurement for g_{sw} model calibration is often to use measurements from a limited number of points in time to determine model parameter values that allow for model prediction across a wide time period (temporal extrapolation). The representativeness of model parameters derived from select subsets of the gas exchange measurements was examined by determining the degree to which they could predict the measured diurnal trend in g_{sw} across multiple days.

Utilizing all data from a given day (seven measurement periods) to determine model parameters and repredict g_{sw} for that day resulted in good agreement. The index of agreement (d_r) for the first day was 0.82 (Fig. S3a) and was 0.77 for the second day (Fig. S3b). Using the data for a given day to derive model parameters and predict the other day (interday extrapolation) significantly decreased performance in one case (d_r of 0.82–0.47; Fig. S3c) while minimally altering performance in the other case (d_r of 0.77–0.73; Fig. S3d). It appears the day with higher conductances could better predict the day with lower conductances but not vice versa.

Performance of whole-day prediction based on parameters derived from one hour's worth of data had mixed results (Fig. S3e,f). For one day, parameters derived from data collected between 10:00 and 11:00 were sufficient to predict the whole day with an equivalent agreement score ($d_r = 0.82$). However, in every other case, using data from only 1 h lowered performance. For one day, the 10:00–11:00 data were better at predicting the whole day than 18:00–19:00 data, but this was the opposite for the other day. Limiting leaf types to only the sunlit or shaded groups of 1 h resulted in complete loss of predictive performance (Fig. S3g,h), demonstrating the importance of sampling a variety of leaves across the PPFD and VPD ranges.

Impacts of nonsteady-state stomatal kinetics

Simulated g_{sw} data incorporating variable stomatal response time constants were generated to examine the impact of stomatal nonequilibrium on the ability to sample underlying stomatal parameters. When stomata respond instantaneously to the environment ($\tau_{gsw} = 0$), every simulated leaf measurement falls exactly on the underlying model surface (Fig. S4a,e). Increasing the stomatal time constant increases scatter about the underlying model surface due to simulated 'measurement' of leaves that are not in equilibrium with their external environment. For example, at a τ of 900 s, the probability of sampling stomatal conductance within 5% of steady state is 33%, while at a τ of 3600 s, that dropped to 22% (Fig. 8).

Real measurements (Fig. S4d,h) contain the superposed impact of stomatal nonequilibrium and leaf-to-leaf variability in underlying physiology (see the 'Underlying stomatal conductance parameters show considerable variability in time and space' section), whereas the simulated dataset only contained nonequilibrium effects. The scatter in the real measured data relative to the fitted model surface is much higher than that of the simulated measurements with similar stomatal time constant ($d_r = 0.65$), which suggests that leaf-to-leaf variability in steady-state stomatal physiology may contribute more to overall scatter in survey measurements than stomatal nonequilibrium.

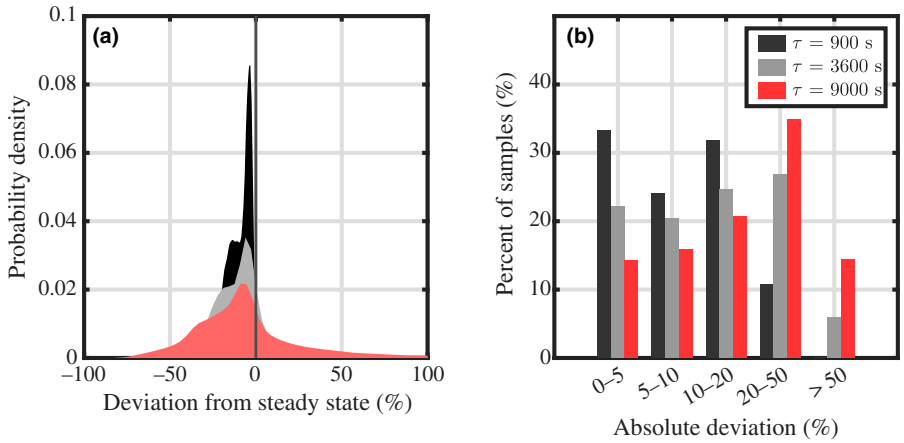

Fig. 8 Stomatal kinetics creates significant deviation from steady state when random survey sampling is used. Simulated data of a 3D redbud tree canopy made of 86 140 leaf patches with known steady-state stomatal parameters was used within a nonsteady-state simulation with realistic variable light fluxes and leaf temperatures to quantify the deviation from steady state of random survey sampling. Results demonstrate that deviation from steady-state increases with an increasing stomatal time constant (τ).

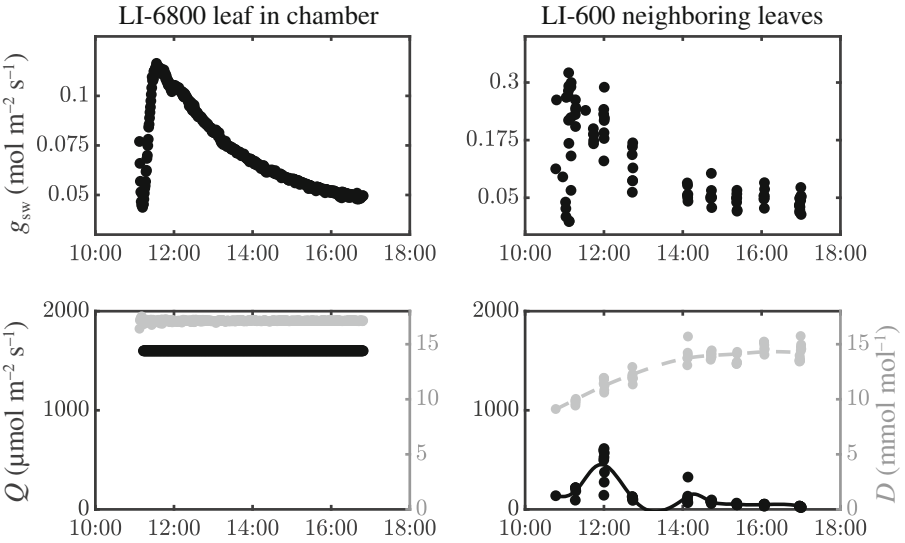

Fig. 9 Test of diurnal effects on stomatal conductance (g_{sw}) in static chamber conditions. A single leaf of Texas red oak (*Quercus buckleyi*) was clamped into a LI-COR LI-6800 chamber from 11:00 to 17:00 PST with a constant photosynthetic photon flux density (Q, black) of 1600 μmol m^{-2} s^{-1}, T_{air} of 22°C and relative humidity (RH) of 35%, which equates to a water vapor mole fraction difference (D, gray) of 17 mmol mol^{-1}. Neighboring leaves were measured over the same time period using a LI-COR LI-600 porometer. Note the y-axis magnitude differences in the top panels.

Impacts of time in the chamber and diurnal effects

To examine the impact of the extended time in the measurement chamber needed to collect steady-state measurements, a leaf was placed in the LI-6800 instrument and kept under constant chamber environment conditions for nearly 6 h. The leaf reached stomatal steady state in *c.* 25 min, but subsequent logarithmic decline in the measured g_{sw} was observed over the next 6 h that reduced stomatal conductance by over half, from *c.* 0.1 to 0.05 mol m^{-2} s^{-1} (Fig. 5). Based on this single leaf measurement alone, it is difficult to determine whether this decline was due to chamber effects or whether the leaf was responding to overall diurnal variation in the tree it was attached to. Performing survey measurements on neighboring leaves throughout the day revealed a similar logarithmic decline in measured g_{sw} (Fig. 9). (The overall magnitude of g_{sw}, presumably due to leaf-to-leaf variability, was larger than that of the leaf that happened to be chosen for the LI-6800 measurement.) This suggests that the observed long-term variation in measured g_{sw} was more likely to be due to diurnal variation in tree water status than from the leaf being subjected to an extended period inside the measurement chamber.

Sample size

A key uncertainty when taking survey measurements is how many samples are needed to sufficiently fit a stomatal conductance model and extract parameters close to the true underlying parameters. We leveraged simulated data with known true parameters and a statistical power analysis to determine the relationship between success rate, acceptable RE threshold, and sample size (Fig. 10).

Success rate, that is the probability of achieving an acceptable fitting error at a given sample size, declines hyperbolically as the error threshold declines (becomes more stringent; Fig. 10a,c). Similarly, success rate increases along an asymptotic hyperbolic curve as sample size increases (Fig. 10b,d). Below roughly 150 samples, the success rate was approximately linear with sample size, above which there was marginal improvement in success rate. For an RE threshold of 20%, a sample size of above 150 yielded a success rate between 70% and 80%. These results were relatively consistent between the real and simulated data (Fig. 10) and were found at a stomatal time constant of *c.* 1800 s. As the time constant was changed in simulation, the success rate for a

New Phytologist

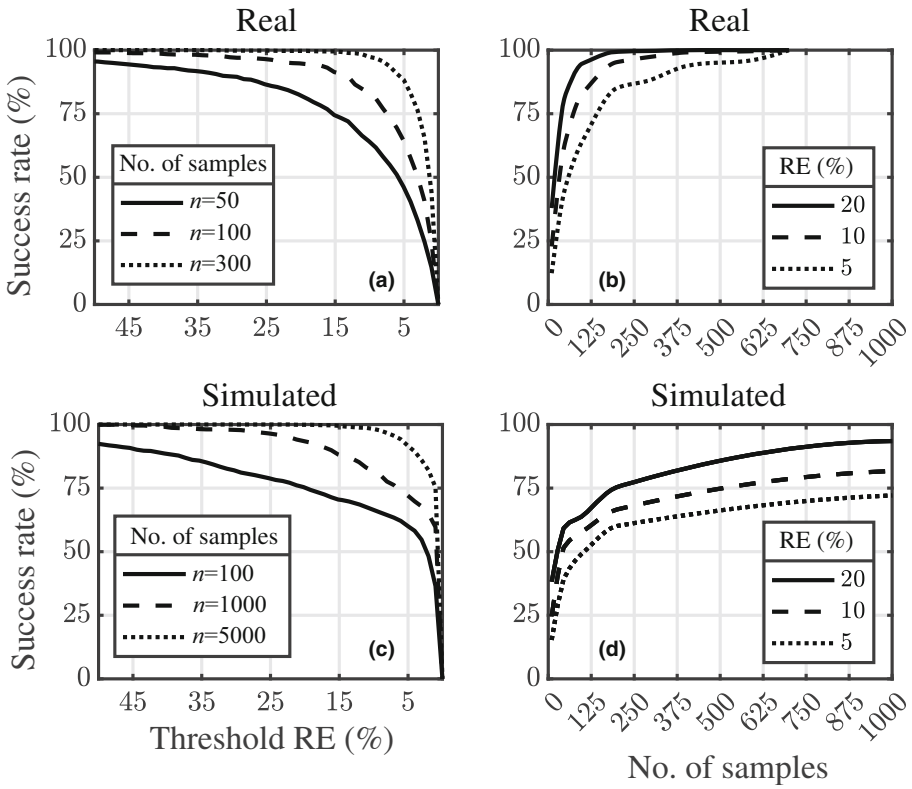

Fig. 10 Statistical power analysis demonstrating the needed sample size for different success rate and error thresholds. The percent relative error (RE), defined as $\frac{|x-\hat{x}|}{x} \cdot 100$, was used as the discrepancy metric between the 'true model' values x and the 'estimate model' values $\hat{x}$. The rate of successfully recovering parameters within a given error threshold declines hyperbolically as success threshold is lowered (a, c). Similarly, the rate of successfully recovering parameters within a given error threshold increases with sample size along an asymptotic hyperbolic curve (b, d). Real nonsteady-state gas exchange data from redbud with a total sample size of 700 leaf patches was used for (a, b), and simulated gas exchange data with a total sample (and population) size of 86 140 leaf patches was used for (c, d). In both cases, the 'true' model parameters are extracted from each case's maximum sample count.

given number of samples changed inversely (Fig. S5). Thus, slower stomata would need higher sampling rates than slower stomata to maintain the same level of confidence in parameter estimation.

Discussion

Underlying stomatal conductance parameters show considerable variability in time and space

In addition to high expected temporal variability in stomatal conductance itself, results illustrated that the underlying parameters that control stomatal responses also vary considerably over time and space. Likely due to the labor-intensive nature of stomatal conductance data collection, robust datasets of stomatal conductance parameters are sparse and existing evidence of the variability of intraspecific parameters across space and time remains mixed with contradictory results (Miner & Bauerle, 2017). In the illustrative study presented in this work, steady-state stomatal conductance of six fully expanded, healthy leaves of the same species exposed to the same environmental conditions varied up to about threefold (e.g. 0.05–-0.14 mol m^{-2} s^{-1} at saturating light and low VPD), with associated high leaf-to-leaf variability in extracted model parameters (Fig. 7; Table 1). While this steady-state leaf-level data produced smooth response curves that facilitated reliable model parameter estimation, choosing only one or a few leaves is unlikely to produce parameters that are representative of the entire plant or canopy. The use of 'survey' measurements is a means of better sampling the spatial variability in stomatal conductance parameters, but the resulting data are noisy and results in increased uncertainty in the extracted model parameters. To mitigate these issues, survey and steady-state measurements could be used in tandem to obtain a robust representation of the shape of response curves, which could be scaled appropriately based on survey data averages (Notes S4; Fig. S6).

In addition to spatial variability in stomatal conductance model parameters, results showed substantial variation in stomatal conductance and its parameters over timescales ranging from hours to months. In some cases, the parameters determined from measurements collected during a given time period could be used to predict stomatal conductance beyond that time period (extrapolation), but in other cases, this failed (Fig. S3). In general, extrapolation appeared most successful when calibration measurements were collected during a period of maximal range in stomatal conductance (Fig. S3). The model appeared unable to make extrapolated predictions where g_{sw} values were generally higher than that of the calibration dataset.

Stomatal conductance is slow to respond to its rapidly varying microenvironment

Stomatal conductance takes significantly more time to reach steady-state than a measurement cuvette takes to reach 'chamber equilibrium' (Fig. 5). In order to associate a measured g_{sw} with a measured PPFD or VPD in a functional manner, tens of minutes or up to an hour is required for stomata to reach steady state.

Table 1 Fitted parameters of the Buckley–Turnbull–Adams stomatal conductance model (Eqn 4) of healthy, fully expanded English walnut (*Juglans regia*) leaves across three colocated trees in Davis, CA, USA, over a season measured in two modes, steady-state and nonsteady-state are reported alongside their coefficient of determination, R^2.

Species	Season	State	Device	Leaf	Tree	$\overline{\psi}_{stem}$	E_m	i_0	k	b	R^2
Walnut	Late	Steady	IRGA	1	1	−1.32	10.6	772	2.88×10^5	46.1	0.985
Walnut	Late	Steady	IRGA	2	1	−1.30	4.18	244	2.99×10^4	11.0	0.982
Walnut	Late	Steady	IRGA	3	1	−1.45	4.96	228	6.19×10^4	16.0	0.978
Walnut	Late	Steady	IRGA	4	2	−1.08	3.07	77.7	9.90×10^3	2.03	0.982
Walnut	Late	Steady	IRGA	5	2	−1.08	3.81	1.22	7.53×10^3	0.51	0.990
Walnut	Late	Steady	IRGA	6	2	−1.11	3.24	159	4.02×10^4	1.23	0.951
Walnut	Late	Non-steady	Porometer	–	3	−1.30	11.9	121	8.49×10^4	14.9	0.493
Walnut	Early	Non-steady	Porometer	–	3	−0.54	10.8	702	9.86×10^4	0.84	0.612

Results exemplify the intraspecific (physiological) and intracanopy (spatiotemporal) variation. The time-averaged stem water potential during the sampling period, $\overline{\psi}_{stem}$, is given in MPa. BTA parameters E_m, i_0, k, and b are given in units of mmol m^{-2} s^{-1}, μmol m^{-2} s^{-1}, μmol m^{-2} s^{-1} mmol mol^{-1}, and mmol mol^{-1}, respectively.

Many studies associating measured g_{sw} with measured chamber conditions do not wait long enough, and thus, the resulting measured g_{sw} is somewhere between the unknown initial ambient state stumbled upon and the final stomatal steady state in response to chamber set points. This can lead to unreliable extracted stomatal conductance model parameters and potentially erroneous experimental results.

For nonsteady-state measurements, this lagged response generates deviation from the underlying relationship of g_{sw} and environmental variables (Figs 6, 8, S4). Using simulations, where the underlying relationship (steady-state BTA model parameters) was known, varying stomatal lag time (quantified by the time constant τ_{gsw}) could reproduce deviation about the true relationship, and the deviation increased with increasing τ. Real data showed significantly more deviation about the best-fit model (Fig. S4). One explanation is that leaves in the real data exhibit variation in their underlying stomatal parameters (this is corroborated by findings discussed above). Another possibility is that the simple time constant approach that implicitly captures the underlying nonsteady-state physics does not accurately represent the time variation in g_{sw} that an explicit, highly resolved biohydromechanical model might in a realistic microenvironment with chaotic trajectories of ambient conditions. We know that this is at least partially true given the 'wrong-way response' (Kappen *et al.*, 1987; Buckley, 2005; Kaiser & Paoletti, 2014). In either case, this deviation leads to difficulties in underlying parameter estimation, but the nonsteady-state deviations can be mitigated by careful sampling considerations.

Protocol modifications for different environments

Our protocols were meant to highlight specific challenges in stomatal conductance measurement and were developed in a Mediterranean climate for plant canopies with accessible leaves. Adaptations for different ecosystems will be needed. For example:

- Tropical forests: High humidities (> 80%) can cause large measurement bias in stomatal conductance using porometers (McDermitt, 1990). IRGA-based systems may be preferred, but VPD ranges attempted in the instrument may need to be reduced.
- Tall canopies: Leaf accessibility will further constrain sampling in tall canopies. Tower platforms, cranes, and lifts can be used to access leaves but dramatically increase sampling costs.
- Arctic/alpine locations: Low ambient temperatures will prohibit portable gas exchange instruments from reaching ideal measurement temperatures described in this study.

Recommendations

Adequate sampling of the spatial variability in underlying leaf-level stomatal parameters is critical in deriving representative canopy-average stomatal conductance model parameters. Thus, survey measurements are needed to sample leaf-to-leaf variability, which is not feasible with steady-state measurements. Measurements of only one to a few leaves, which is characteristic of steady-state measurements, are likely to result in unrepresentative model parameters. Confidence in extracted model parameters increases sharply with sample size at first until beginning to level off. A statistical power analysis on field data and realistic simulated data with known underlying parameters suggested that *c.* 150 random samples in our case was the beginning of diminishing marginal returns of the rate of successfully extracting model parameters (Fig. 10). Depending on the application and the desired throughput speed, different sample sizes may be considered, but below these apparent 'inflection' points confidence in the extracted parameters drops precipitately. Based on presented findings, we recommend a minimum survey sample size on the order of 100 to balance throughput and performance. However, this scales up with increased stomatal time constants (Fig. S5). Our datasets primarily consisted of perennials with moderate stomatal response times. Species that exhibit faster stomatal response times (e.g. prominent annual crops *Oryza sativa* and *Zea mays*; McAusland *et al.*, 2016) would require fewer samples to achieve the same confidence in parameter extraction, all else equal.

In order to maximize representativeness of derived stomatal parameters, survey measurements should be collected during

periods containing maximum stomatal conductance, which are periods of simultaneously high light, low VPD, high soil moisture, and low overall stress. This tends to occur late morning when light is near its maximum, but air temperature and humidity are still several hours away from reaching their respective maximum and minimum. Choose healthy, fully expanded leaves and avoid periods of stress due to heat, drought, disease, or pests. Note that stomata of some species exhibit strong circadian rhythms and may be unresponsive to environmental conditions and instead driven primarily by internal signals; unless included in a model in a parameterizable way, times of day strongly influenced by circadian patterns should be avoided. This is typically the early morning and late evening.

When sampling leaves for survey measurements, it is critical to choose leaves with as wide a range of light and VPD combinations as possible, while also limiting measurements to leaves that do not appear to have recently changed their light level. The wide range of light and VPD combinations is necessary to explore the model surface and thus reliably describe environmental responses. Choosing leaves that have maintained a similar light level for a prolonged period maximizes the chances that stomata are close to equilibrium with the environment. Each survey measurement should be performed as quickly as possible to avoid significant stomatal responses to the instrument chamber environment before measurement.

Steady-state response curve data can be used in tandem with survey measurements to more accurately represent the shapes of stomatal response curves and the parameters that describe them (but should generally not be used on their own for calibration if sparse in number). It is critical when collecting stomatal response curve data to wait until stomatal steady state is reached at each light and VPD set point before recording the measurement, which bears a significant time cost. This limits the amount of leaf-to-leaf variation that is able to be captured and hinders the representativeness of the calibrated parameters beyond the sample of leaves measured. One compromise is to collect a few response curves, but then scale them using the variation observed in many survey measurements. This is easily achieved by dividing by their maximum and multiplying by some derived statistic from the survey data, such as the mean, maximum, 95th percentile, or a random sample from a distribution (Fig. S6). We demonstrate this process in Notes S4.

Canopy-average stomatal conductance model parameters can exhibit significant seasonal changes. It may be necessary to derive separate parameter sets based on plant growth stages (e.g. vegetative growth, reproductive growth, and senescence) in order to facilitate reliable model predictions over seasonal timescales. Furthermore, if parameterizing more resolute models that assign individual leaves unique parameters based on additional measurements of leaf age, position in the canopy, integrated light history, temperature acclimation, diurnal effects, etc. (e.g. Matthews *et al.*, 2018; Oliver *et al.*, 2022), then the number of samples may need to grow exponentially with the number of additional parameters included in the model due to the exponentially expanding dimensional volume of the parameter space.

Three sample protocols for measurements and model calibration are given in Rizzo & Bailey (2025a) with different scenarios depending on available time and instrumentation. The protocols were developed in a temperate climate but are meant to serve as examples to be easily adjusted for alternative environmental conditions. Software for robust calibration of select stomatal conductance models has been incorporated into the PhoTorch Python package for plant physiological model fitting (https://www.github.com/GEMINI-Breeding/photorch).

Acknowledgments

This work was supported by the US Department of Agriculture National Institute of Food and Agriculture (Hatch project no. 7003146) and US National Science Foundation (grant nos. IOS 2047628 and 2307341). We acknowledge Miguel H. Ochoa for collection of several fruit tree steady-state stomatal response curves displayed within the data of Fig. 2.

Competing interests

None declared.

Author contributions

KTR was involved in conceptualization, data curation, formal analysis, investigation, methodology, software, visualization, writing – original draft. TL was involved in data curation, software, writing – review and editing. TNB was involved in resources, writing – review and editing. BNB was involved in conceptualization, funding acquisition, methodology, project administration, resources, software, supervision, writing – original draft.

ORCID

Brian N. Bailey https://orcid.org/0000-0003-1919-2324
Thomas N. Buckley https://orcid.org/0000-0001-7610-7136
Kyle T. Rizzo https://orcid.org/0009-0001-3864-4106

Data availability

The data that support the findings of this study are openly available in Dryad at doi: 10.5061/dryad.5x69p8djr.

References

Acharya BR, Assmann SM. 2009. Hormone interactions in stomatal function. *Plant Molecular Biology* **69**: 451–462.

Akima H. 1970. A new method of interpolation and smooth curve fitting based on local procedures. *Journal of the ACM* **17**: 589–602.

Anderegg WR. 2015. Spatial and temporal variation in plant hydraulic traits and their relevance for climate change impacts on vegetation. *New Phytologist* **205**: 1008–1014.

Arneth A, Lloyd J, Šantrůčková H, Bird M, Grigoryev S, Kalaschnikov YN, Gleixner G, Schulze ED. 2002. Response of central siberian scots pine to soil

water deficit and long-term trends in atmospheric CO_2 concentration. *Global Biogeochemical Cycles* **16**: 5-1–5-13.

Atkinson C, Winner W, Mooney H. 1986. A field portable gas-exchange system for measuring carbon dioxide and water vapour exchange rates of leaves during fumigation with SO2. *Plant, Cell & Environment* **9**: 711–719.

Bailey BN. 2019. Helios: A scalable 3D plant and environmental biophysical modelling framework. *Frontiers in Plant Science* **10**: 1185.

Ball JT, Woodrow IE, Berry JA. 1987. A model predicting stomatal conductance and its contribution to the control of photosynthesis under different environmental conditions. In: *Progress in photosynthesis research: volume 4 proceedings of the VIIth international congress on photosynthesis providence, Rhode Island, USA, August 10–15, 1986*. Berlin, Heidelberg: Springer, 221–224.

Bassiouni M, Vico G. 2021. Parsimony vs predictive and functional performance of three stomatal optimization principles in a big-leaf framework. *New Phytologist* **231**: 586–600.

Bernacchi C, Singsaas E, Pimentel C, Portis A Jr, Long SP. 2001. Improved temperature response functions for models of rubisco-limited photosynthesis. *Plant, Cell & Environment* **24**: 253–259.

Bernardo EL, Sales CRG, Cubas LA, Vath RL, Kromdijk J. 2023. A comparison of stomatal conductance responses to blue and red light between C_3 and C_4 photosynthetic species in three phylogenetically-controlled experiments. *Frontiers in Plant Science* **14**: 1253976.

Berry JA. 2012. There ought to be an equation for that. *Annual Review of Plant Biology* **63**: 1–17.

Bertolino LT, Caine RS, Gray JE. 2019. Impact of stomatal density and morphology on water-use efficiency in a changing world. *Frontiers in Plant Science* **10**: 225.

Brainard L, Eching S, Mollenberndt D, California Department of Water Resources. 1996. CIMIS, California Irrigation Management Information System, urban resource book. State of California, The Resources Agency, Department of Water Resources.

Browne M, Bartlett MK, Henry C, Jarrahi M, John G, Scoffoni C, Yardimci NT, Sack L. 2023. Low baseline intraspecific variation in leaf pressure-volume traits: biophysical basis and implications for spectroscopic sensing. *Physiologia Plantarum* **175**: e13974.

Buckley TN. 2005. The control of stomata by water balance. *New Phytologist* **168**: 275–292.

Buckley TN. 2017. Modeling stomatal conductance. *Plant Physiology* **174**: 572–582.

Buckley TN. 2019. How do stomata respond to water status? *New Phytologist* **224**: 21–36.

Buckley TN, Farquhar GD, Mott KA. 1999. Carbon-water balance and patchy stomatal conductance. *Oecologia* **118**: 132–143.

Buckley TN, Mott KA, Farquhar GD. 2003. A hydromechanical and biochemical model of stomatal conductance. *Plant, Cell & Environment* **26**: 1767–1785.

Buckley TN, Turnbull TL, Adams MA. 2012. Simple models for stomatal conductance derived from a process model: cross-validation against sap flux data. *Plant, Cell & Environment* **35**: 1647–1662.

Busch FA, Ainsworth EA, Amtmann A, Cavanagh AP, Driever SM, Ferguson JN, Kromdijk J, Lawson T, Leakey ADB, Matthews JSA *et al.* 2024. A guide to photosynthetic gas exchange measurements: fundamental principles, best practice and potential pitfalls. *Plant, Cell & Environment* **47**: 3344–3364.

Cardon Z, Mott K, Berry J. 1994. Dynamics of patchy stomatal movements, and their contribution to steady-state and oscillating stomatal conductance calculated using gas-exchange techniques. *Plant, Cell & Environment* **17**: 995–1007.

Chazdon RL, Pearcy RW. 1991. The importance of sunflecks for forest understory plants. *Bioscience* **41**: 760–766.

Cowan IR. 1972. Oscillations in stomatal conductance and plant functioning associated with stomatal conductance: observations and a model. *Planta* **106**: 185–219.

Cowan IR, Farquhar GD. 1977. Stomatal function in relation to leaf metabolism and environment. *Symposia of the Society for Experimental Biology* **31**: 471–505.

Crous KY, Middleby KB, Cheesman AW, Bouet AY, Schiffer M, Liddell MJ, Barton CV, Cernusak LA. 2025. Leaf warming in the canopy of mature tropical trees reduced photosynthesis due to downregulation of photosynthetic capacity and reduced stomatal conductance. *New Phytologist* **245**: 1421–1436.

Damour G, Simonneau T, Cochard H, Urban L. 2010. An overview of models of stomatal conductance at the leaf level. *Plant, Cell & Environment* **33**: 1419–1438.

Dodd AN, Salathia N, Hall A, Kévei E, Tóth R, Nagy F, Hibberd JM, Millar AJ, Webb AA. 2005. Plant circadian clocks increase photosynthesis, growth, survival, and competitive advantage. *Science* **309**: 630–633.

Drake PL, Froend RH, Franks PJ. 2013. Smaller, faster stomata: scaling of stomatal size, rate of response, and stomatal conductance. *Journal of Experimental Botany* **64**: 495–505.

Fan LM, Zhao Z, Assmann SM. 2004. Guard cells: a dynamic signaling model. *Current Opinion in Plant Biology* **7**: 537–546.

Faralli M, Matthews J, Lawson T. 2019. Exploiting natural variation and genetic manipulation of stomatal conductance for crop improvement. *Current Opinion in Plant Biology* **49**: 1–7.

Farquhar GD, Sharkey TD. 1982. Stomatal conductance and photosynthesis. *Annual Review of Plant Physiology* **33**: 317–345.

Farquhar GD, von Caemmerer S, Berry JA. 1980. A biochemical model of photosynthetic CO_2 assimilation in leaves of C_3 species. *Planta* **149**: 78–90.

Field C, Berry JA, Mooney HA. 1982. A portable system for measuring carbon dioxide and water vapour exchange of leaves. *Plant, Cell & Environment* **5**: 179–186.

Frank A. 1981. Effect of leaf age and position on photosynthesis and stomatal conductance of forage grasses 1. *Agronomy Journal* **73**: 70–74.

Grantz DA, Zeiger E. 1986. Stomatal responses to light and leaf-air water vapor pressure difference show similar kinetics in sugarcane and soybean. *Plant Physiology* **81**: 865–868.

Gray J, Dunn J. 2024. Optimizing crop plant stomatal density to mitigate and adapt to climate change. *Cold Spring Harbor Perspectives in Biology* **16**: a041672.

Grisafi F, DeJong TM, Tombesi S. 2022. Fruit tree crop models: an update. *Tree Physiology* **42**: 441–457.

Grossiord C, Buckley TN, Cernusak LA, Novick KA, Poulter B, Siegwolf RT, Sperry JS, McDowell NG. 2020. Plant responses to rising vapor pressure deficit. *New Phytologist* **226**: 1550–1566.

Gu L, Pallardy SG, Tu K, Law BE, Wullschleger SD. 2010. Reliable estimation of biochemical parameters from C_3 leaf photosynthesis–intercellular carbon dioxide response curves. *Plant, Cell & Environment* **33**: 1852–1874.

Harmer SL. 2009. The circadian system in higher plants. *Annual Review of Plant Biology* **60**: 357–377.

Hennessey TL, Freeden AL, Field CB. 1993. Environmental effects on circadian rhythms in photosynthesis and stomatal opening. *Planta* **189**: 369–376.

Hetherington AM, Woodward FI. 2003. The role of stomata in sensing and driving environmental change. *Nature* **424**: 901–908.

Hiyama T, Kochi K, Kobayashi N, Sirisampan S. 2005. Seasonal variation in stomatal conductance and physiological factors observed in a secondary warm-temperate forest. In: *Forest ecosystems and environments: scaling up from shoot module to watershed*. Berlin, Heidelberg: Springer, 97–110.

Iino M, Ogawa T, Zeiger E. 1985. Kinetic properties of the blue-light response of stomata. *Proceedings of the National Academy of Sciences, USA* **82**: 8019–8023.

Jefferson JL, Maxwell RM, Constantine PG. 2017. Exploring the sensitivity of photosynthesis and stomatal resistance parameters in a land surface model. *Journal of Hydrometeorology* **18**: 897–915.

Jones HG. 1998. Stomatal control of photosynthesis and transpiration. *Journal of Experimental Botany* **49**: 387–398.

Jones JW, Hoogenboom G, Porter CH, Boote KJ, Batchelor WD, Hunt LA, Wilkens PW, Singh U, Gijsman AJ, Ritchie JT. 2003. The DSSAT cropping system model. *European Journal of Agronomy* **18**: 235–265.

Kaiser H, Paoletti E. 2014. Dynamic stomatal changes. In: *Trees in a changing environment: ecophysiology, adaptation, and future survival*. Berlin, Heidelberg: Springer, 61–82.

Kappen L, Andresen G, Lösch R. 1987. *In situ* observations of stomatal movements. *Journal of Experimental Botany* **38**: 126–141.

Kay JE, Deser C, Phillips A, Mai A, Hannay C, Strand G, Arblaster JM, Bates S, Danabasoglu G, Edwards J *et al.* 2015. The Community Earth System Model (CESM) large ensemble project: a community resource for studying climate change in the presence of internal climate variability. *Bulletin of the American Meteorological Society* **96**: 1333–1349.

Kim SH, Lieth JH. 2003. A coupled model of photosynthesis, stomatal conductance and transpiration for a rose leaf (*Rosa hybrida* L.). *Annals of Botany* **91**: 771–781.

Kimura K, Fushimi E, Kumagai E, Nomura K, Matsunami T, Konno S, Maruyama A. 2025. Estimating leaf CO_2 assimilation in C_3 plants using a handheld porometer with chlorophyll fluorometer in field conditions. *Plant, Cell & Environment* **48**: 7213–7224.

Kirschbaum MUF, Gross LJ, Pearcy RW. 1988. Observed and modelled stomatal responses to dynamic light environments in the shade plant alocasia macrorrhiza. *Plant, Cell & Environment* **11**: 111–121.

Krayenhoff ES, Jiang T, Christen A, Martilli A, Oke TR, Bailey BN, Nazarian N, Voogt JA, Giometto MG, Stastny A *et al.* 2020. A multi-layer urban canopy meteorological model with trees (BEP-Tree): street tree impacts on pedestrian-level climate. *Urban Climate* **32**: 100590.

Lamoureux L, Sacco D, Risse PA, Lovisolo C. 2017. Factors influencing stomatal conductance in response to water availability in grapevine: a meta-analysis. *Physiologia Plantarum* **159**: 468–482.

Lawson T, Matthews J. 2020. Guard cell metabolism and stomatal function. *Annual Review of Plant Biology* **71**: 273–302.

Lawson T, von Caemmerer S, Baroli I. 2011. Photosynthesis and stomatal behaviour. *Progress in Botany* **72**: 265–304.

Lei T, Rizzo KT, Bailey BN. 2025. PhoTorch: a robust and generalized biochemical photosynthesis model fitting package based on pytorch. *Photosynthesis Research* **163**: 21.

Leuning R. 1995. A critical appraisal of a combined stomatal-photosynthesis model for C3 plants. *Plant, Cell & Environment* **18**: 339–355.

Leuning R, Dunin F, Wang YP. 1998. A two-leaf model for canopy conductance, photosynthesis and partitioning of available energy. II. Comparison with measurements. *Agricultural and Forest Meteorology* **91**: 113–125.

Mansfield TA. 2012. Hormones as regulators of water balance. In: Davies P, ed. *Plant Hormones and their role in plant growth and development*. Dordrecht, The Netherlands: Springer Netherlands, 411–430.

Marenco RA, Siebke K, Farquhar GD, Ball MC. 2006. Hydraulically based stomatal oscillations and stomatal patchiness in *Gossypium hirsutum*. *Functional Plant Biology* **33**: 1103–1113.

Maruyama A, Kuwagata T. 2008. Diurnal and seasonal variation in bulk stomatal conductance of the rice canopy and its dependence on developmental stage. *Agricultural and Forest Meteorology* **148**: 1161–1173.

Matsumoto K, Ohta T, Tanaka T. 2005. Dependence of stomatal conductance on leaf chlorophyll concentration and meteorological variables. *Agricultural and Forest Meteorology* **132**: 44–57.

Matthews JS, Vialet-Chabrand S, Lawson T. 2018. Acclimation to fluctuating light impacts the rapidity of response and diurnal rhythm of stomatal conductance. *Plant Physiology* **176**: 1939–1951.

Matthews JS, Vialet-Chabrand S, Lawson T. 2020. Role of blue and red light in stomatal dynamic behaviour. *Journal of Experimental Botany* **71**: 2253–2269.

Mayanja IK, Yun H, Bailey BN. 2025. Automated calibration of stomatal conductance models from thermal imagery by leveraging synthetic images generated from Helios 3D biophysical model simulations. *Journal of Experimental Botany* **77**: 312–329.

McAdam SA, Brodribb TJ. 2015. The evolution of mechanisms driving the stomatal response to vapor pressure deficit. *Plant Physiology* **167**: 833–843.

McAusland L, Vialet-Chabrand S, Davey P, Baker NR, Brendel O, Lawson T. 2016. Effects of kinetics of light-induced stomatal responses on photosynthesis and water-use efficiency. *New Phytologist* **211**: 1209–1220.

McDermitt D. 1990. Sources of error in the estimation of stomatal conductance and transpiration from porometer data. *HortScience* **25**: 1538–1548.

Medlyn BE, Duursma RA, Eamus D, Ellsworth DS, Prentice IC, Barton CV, Crous KY, De Angelis P, Freeman M, Wingate L. 2011. Reconciling the optimal and empirical approaches to modelling stomatal conductance. *Global Change Biology* **17**: 2134–2144.

Miner GL, Bauerle WL. 2017. Seasonal variability of the parameters of the Ball–Berry model of stomatal conductance in maize (*Zea mays* L.) and sunflower (*Helianthus annuus* L.) under well-watered and water-stressed conditions. *Plant, Cell & Environment* **40**: 1874–1886.

Mott KA. 1988. Do stomata respond to CO_2 concentrations other than intercellular? *Plant Physiology* **86**: 200–203.

Mott KA, Buckley TN. 1998. Stomatal heterogeneity. *Journal of Experimental Botany* **49**: 407–417.

Mott KA, O'Leary JW. 1984. Stomatal behavior and CO_2 exchange characteristics in amphistomatous leaves. *Plant Physiology* **74**: 47–51.

Nguyen TH, Silva-Alvim FAL, Hills A, Blatt MR. 2023. OnGuard3e: A predictive, ecophysiology-ready tool for gas exchange and photosynthesis research. *Plant, Cell & Environment* **46**: 3644–3658.

Nilson SE, Assmann SM. 2007. The control of transpiration. Insights from Arabidopsis. *Plant Physiology* **143**: 19–27.

Oleson KW, Lawrence DM, Gordon B, Flanner MG, Kluzek E, Peter J, Levis S, Swenson SC, Thornton E, Feddema J. 2010. Technical description of version 4.0 of the Community Land Model (CLM).

Oliver RJ, Mercado LM, Clark DB, Huntingford C, Taylor CM, Vidale PL, McGuire PC, Todt M, Folwell S, Shamsudheen Semeena V *et al.* 2022. Improved representation of plant physiology in the JULES-vn5.6 land surface model: photosynthesis, stomatal conductance and thermal acclimation. *Geoscientific Model Development Discussions* **2022**: 1–41.

Ooba M, Takahashi H. 2003. Effect of asymmetric stomatal response on gas-exchange dynamics. *Ecological Modelling* **164**: 65–82.

Ozeki K, Miyazawa Y, Sugiura D. 2022. Rapid stomatal closure contributes to higher water use efficiency in major C_4 compared to C_3 poaceae crops. *Plant Physiology* **189**: 188–203.

Parkinson K, Day W, Leach J. 1980. A portable system for measuring the photosynthesis and transpiration of graminaceous leaves. *Journal of Experimental Botany* **31**: 1441–1453.

Peak D, Hogan MT, Mott KA. 2023. Stomatal patchiness and cellular computing. *Proceedings of the National Academy of Sciences, USA* **120**: e2220270120.

Ponce de León MA, Bailey BN. 2021. A 3D model for simulating spatial and temporal fluctuations in grape berry temperature. *Agricultural and Forest Meteorology* **306**: 108431.

Rayment M, Loustau D, Jarvis P. 2000. Measuring and modeling conductances of black spruce at three organizational scales: shoot, branch and canopy. *Tree Physiology* **20**: 713–723.

Rebetzke G, Read J, Barbour M, Condon A, Rawson H. 2000. A hand-held porometer for rapid assessment of leaf conductance in wheat. *Crop Science* **40**: 277–280.

de Resco Dios V, Anderegg WR, Li X, Tissue DT, Bahn M, Landais D, Milcu A, Yao Y, Nolan RH, Roy J *et al.* 2020. Circadian regulation does not optimize stomatal behaviour. *Plants* **9**: 1091.

de Resco Dios V, Díaz-Sierra R, Goulden ML, Barton CV, Boer MM, Gessler A, Ferrio JP, Pfautsch S, Tissue DT. 2013. Woody clockworks: circadian regulation of night-time water use in *Eucalyptus globulus*. *New Phytologist* **200**: 743–752.

de Resco Dios V, Gessler A, Ferrio JP, Alday JG, Bahn M, Del Castillo J, Devidal S, García-Muñoz S, Kayler Z, Landais D *et al.* 2016. Circadian rhythms have significant effects on leaf-to-canopy scale gas exchange under field conditions. *GigaScience* **5**: 43.

Rizzo KT, Bailey BN. 2025a. Protocol for leaf-level gas exchange measurement for stomatal conductance model calibration. doi: 10.17504/protocols.io.j8nlky52wg5r/v2.

Rizzo KT, Bailey BN. 2025b. A psychrometric temperature correction for the positive bias observed in stomatal conductance measured by the open flow-through LI-600 porometer. *Plant, Cell & Environment*: 1–12. doi: 10.1111/pce.70304.

Sabot ME, De Kauwe MG, Pitman AJ, Medlyn BE, Ellsworth DS, Martin-StPaul NK, Wu J, Choat B, Limousin JM, Mitchell PJ *et al.* 2022. One stomatal model to rule them all? Toward improved representation of carbon and water exchange in global models. *Journal of Advances in Modeling Earth Systems* **14**: e2021MS002761.

Sharkey TD, Raschke K. 1981. Separation and measurement of direct and indirect effects of light on stomata. *Plant Physiology* **68**: 33–40.

Shimazaki KI, Doi M, Assmann SM, Kinoshita T. 2007. Light regulation of stomatal movement. *Annual Review of Plant Biology* **58**: 219–247.

Shimshi D. 1977. A fast-reading viscous flow leaf porometer. *New Phytologist* **78**: 593–598.

Steppe K, Dzikiti S, Lemeur R, Milford JR. 2006. Stomatal oscillations in orange trees under natural climatic conditions. *Annals of Botany* **97**: 831–835.

Sun Z, Wang X, Song Y, Li Q, Song J, Cai J, Zhou Q, Zhong Y, Jin S, Jiang D. 2023. StomataTracker: revealing circadian rhythms of wheat stomata with in-situ video and deep learning. *Computers and Electronics in Agriculture* **212**: 108120.

Toro G, Flexas J, Escalona JM. 2019. Contrasting leaf porometer and infra-red gas analyser methodologies: an old paradigm about the stomatal conductance measurement. *Theoretical and Experimental Plant Physiology* **31**: 483–492.

Turner NC. 1991. Measurement and influence of environmental and plant factors on stomatal conductance in the field. *Agricultural and Forest Meteorology* **54**: 137–154.

Tyree M, Wilmot T. 1990. Errors in the calculation of evaporation and leaf conductance in steady-state porometry: the importance of accurate measurement of leaf temperature. *Canadian Journal of Forest Research* **20**: 1031–1035.

Verhoef A. 1997. The effect of temperature differences between porometer head and leaf surface on stomatal conductance measurements. *Plant, Cell & Environment* **20**: 641–646.

Vialet-Chabrand S, Lawson T. 2019. Dynamic leaf energy balance: deriving stomatal conductance from thermal imaging in a dynamic environment. *Journal of Experimental Botany* **70**: 2839–2855.

Vialet-Chabrand SR, Matthews JS, McAusland L, Blatt MR, Griffiths H, Lawson T. 2017. Temporal dynamics of stomatal behavior: modeling and implications for photosynthesis and water use. *Plant Physiology* **174**: 603–613.

Vos J, Oyarzun P. 1987. Photosynthesis and stomatal conductance of potato leaves—effects of leaf age, irradiance, and leaf water potential. *Photosynthesis Research* **11**: 253–264.

Wang H, Ma M, Xie Y, Wang X, Wang J. 2014. Parameter inversion estimation in photosynthetic models: impact of different simulation methods. *Photosynthetica* **52**: 233–246.

Wang YP, Jarvis PG. 1990. Description and validation of an array model – MAESTRO. *Agricultural and Forest Meteorology* **51**: 257–280.

Weatherley PE. 1966. A porometer for use in the field. *New Phytologist* **65**: 376–387.

Willmer C, Fricker M. 1996. *Stomata, vol. 2.* Dordrecht, The Netherlands: Springer Science & Business Media.

Willmott CJ, Robeson SM, Matsuura K. 2012. A refined index of model performance. *International Journal of Climatology* **32**: 2088–2094.

Zhang N, Berman SR, Joubert D, Vialet-Chabrand S, Marcelis LF, Kaiser E. 2022. Variation of photosynthetic induction in major horticultural crops is mostly driven by differences in stomatal traits. *Frontiers in Plant Science* **13**: 860229.

Zhou S, Duursma RA, Medlyn BE, Kelly JW, Prentice IC. 2013. How should we model plant responses to drought? An analysis of stomatal and non-stomatal responses to water stress. *Agricultural and Forest Meteorology* **182**: 204–214.

Supporting Information

Additional Supporting Information may be found online in the Supporting Information section at the end of the article.

Fig. S1 Comparison of stomatal conductance model fits across three measurement approaches, showing population-level and leaf-level performance for four commonly used stomatal conductance models.

Fig. S2 Time-resolved snapshots of simulated stomatal conductance in a three-dimensional eastern redbud canopy model driven by measured environmental conditions.

Fig. S3 Evaluation of the representativeness of stomatal conductance model parameters calibrated from different temporal and spatial data subsets in predicting diurnal canopy-scale behavior.

Fig. S4 Simulated and measured stomatal conductance responses to absorbed light and vapor pressure deficit, illustrating the influence of stomatal time constants on deviations from steady state.

Fig. S5 Statistical power analysis demonstrating the increased sampling effort required to recover steady-state stomatal conductance relationships as stomatal response times increase.

Fig. S6 Example of rescaling a steady-state stomatal light response curve using survey-based statistics to better represent canopy-level variability.

Notes S1 Description of the inversion approach used to estimate net photosynthesis and internal leaf $CO2$ from porometer measurements using pre-fitted Farquhar–von Caemmerer–Berry photosynthesis model parameters.

Notes S2 Formulation and implementation details of the nonlinear mixed-effects modeling framework used to estimate population-level and leaf-level stomatal conductance model parameters.

Notes S3 Technical description of the three-dimensional plant biophysical modeling framework used to simulate coupled light interception, energy balance, and stomatal conductance dynamics.

Notes S4 Method for rescaling steady-state stomatal conductance response curves using survey-derived statistics to better represent canopy-level variability.

Table S1 Species-specific Farquhar–von Caemmerer–Berry photosynthesis model parameters used for porometer-based assimilation inversion in walnut leaves.

Table S2 List of plant species included in the study, indicating response state classification and associated figures.

Table S3 Ball–Woodrow–Berry stomatal conductance model parameter estimates and goodness-of-fit metrics derived from porometer and infrared gas analyzer measurements.

Table S4 Medlyn *et al.* stomatal conductance model parameter estimates and goodness-of-fit metrics across measurement methods and modeling approaches.

Table S5 Ball–Berry–Leuning stomatal conductance model fitting results comparing population-level and leaf-level parameterization strategies.

Table S6 Buckley–Turnbull–Adams stomatal conductance model fitting results illustrating differences between survey-based and steady-state calibration approaches.

Please note: Wiley is not responsible for the content or functionality of any Supporting Information supplied by the authors. Any queries (other than missing material) should be directed to the *New Phytologist* Central Office.